



Article

Induction and Characterisation of Lignocellulolytic Activities from Novel Deep-Sea Fungal Secretomes

Bronwyn Dowd * and Maria G. Tuohy *

Molecular Glycobiotechnology Group, Biochemistry, School of Biological and Chemical Sciences, Ryan Institute and MaREI, University of Galway, H91 TK33 Galway, Ireland

* Correspondence: b.dowd1@nuigalway.ie (B.D.); maria.tuohy@universityofgalway.ie (M.G.T.)

Abstract: Fungi are increasingly recognised as being able to inhabit extreme environments. The deep sea is considered an extreme environment because of its low temperatures, high hydrostatic and lithostatic pressures, 3.5% salinity, and low oxygen, nutrient and light availability. Fungi inhabiting the deep sea may have evolved to produce proteins that allow them to survive these conditions. Investigation and characterisation of fungal lignocellulolytic enzymes from extreme environments like the deep sea is needed, as they may have unusual adaptations that would be useful in industry. This work, therefore, aimed to profile in detail the lignocellulolytic capabilities of fungi isolated from deep-sea sediments in the Atlantic Ocean, and a comparative lignocellulolytic terrestrial isolate. The isolates were strains of *Emericellopsis maritima*, *Penicillium chrysogenum*, *P. antarcticum* and *Talaromyces stollii*. Lignocellulolytic enzyme induction was achieved using liquid-state fermentation (LSF) with wheat bran as the main carbon source, while enzyme characteristics were evaluated using biochemical assays and gel-based proteomics. This study revealed that the isolates were halotolerant, produced xylanase over wide pH and temperature ranges, and produced a variety of glycoside hydrolase and feruloyl esterase activities. The *T. stollii* secretome demonstrated remarkable levels of exo-glycoside hydrolase activity, with xylanase activity optimum between pH 1.5–6.0 and temperatures between 1–60 °C, making this isolate an ideal candidate for biotechnological applications. This study is the first to quantitatively characterise xylanase activities and exo-glycoside hydrolase activities secreted by *E. maritima*, *P. antarcticum* and a marine *T. stollii* strain. This study is also the first to quantitatively characterise xylanase activities by a marine strain of *P. chrysogenum* during LSF.



Citation: Dowd, B.; Tuohy, M.G. Induction and Characterisation of Lignocellulolytic Activities from Novel Deep-Sea Fungal Secretomes. *Fermentation* **2023**, *9*, 780. <https://doi.org/10.3390/fermentation9090780>

Academic Editor: Antonella Costantini

Received: 1 July 2023

Revised: 11 August 2023

Accepted: 21 August 2023

Published: 23 August 2023



Copyright: © 2023 by the authors. Licensee MDPI, Basel, Switzerland. This article is an open access article distributed under the terms and conditions of the Creative Commons Attribution (CC BY) license (<https://creativecommons.org/licenses/by/4.0/>).

Keywords: lignocellulose-degrading enzymes; enzyme induction; marine fungi; proteomics; xylanase; *Penicillium chrysogenum*; *Penicillium antarcticum*; *Talaromyces stollii*; *Emericellopsis maritima*; CAZymes

1. Introduction

In recent years, interest in the discovery and characterisation of novel bioactive compounds and enzymes from microorganisms inhabiting extreme environments has increased. Extreme environments such as the desert, the Antarctic and Arctic poles, and the deep sea have been explored to this end [1]. While bacteria and archaea from extreme environments have been investigated extensively, fungi are now gaining more attention, as they are increasingly recognised as being able to inhabit severely inhospitable conditions, showing resilience and adaptability that may surpass that of prokaryotes [2–4].

The deep sea is considered an extreme environment because temperatures go below 5 °C, the water column pressure is high (increase in 105 Pascal for every 10 m increase in depth) and the salinity is at 3.5%. Additionally, the availability of oxygen, nutrients and light is low. These conditions place extreme physiological pressure on microbial growth and metabolism.

Due to the nature of these environments, it is likely that fungi inhabiting the deep sea have evolved to produce proteins that allow them to survive in these extreme conditions, thus having a biological advantage over terrestrial fungi [5–7]. Furthermore, it has been

shown that cultured isolates from the deep sea do not have any practical disadvantage to their terrestrial counterparts in terms of their ability to grow and be cultured (no special conditions are required), and, therefore, if the strains prove to be useful, for example, in industrial applications, there would be no practical issues when compared to terrestrial strains [7].

Fungi from the deep sea have been found in many studies to produce novel bioactive compounds of medical interest such as polyketides [8], terpenoids [9], alkaloids and steroids [10]. Less attention, however, has been given to their ability to produce lignocellulose-degrading enzymes.

Fungi are well established as excellent producers of lignocellulolytic enzymes [11]. The most abundant source of biomass on the planet is lignocellulose [12], which is made up of cellulose, hemicellulose and lignin and forms a recalcitrant matrix [13,14]. With the increase in demand for more efficient, powerful and diverse lignocellulose-degrading enzymes in industry, investigation and characterisation of fungal lignocellulolytic enzymes from extreme environments like the deep sea is needed, as they may prove to have unusual adaptations that would be useful in biotechnological applications [7]. For example, if the lignocellulose matrix could be degraded in a cost- and energy-efficient and environmentally friendly manner, it would make it possible to use abundant lignocellulosic wastes as feedstocks for the production of biofuels like methane or ethanol on a far wider scale than they are at present [15,16].

Other applications for novel lignocellulolytic enzymes from the deep sea could be in the preparation of paper pulp, which is carried out under alkaline conditions. The ocean has an average pH of 8.1 and enzymes functioning in alkaline conditions from deep-sea fungi have been discovered and characterised [17–19]. Lignocellulolytic and proteolytic enzymes from deep-sea fungi have also been reported with functionality at low temperatures [7,18], which could reduce the cost of heating during bioprocesses in the industry. However, it appears that we have just uncovered ‘the tip of the iceberg’, with relatively few studies of fungal deep-sea lignocellulolytic enzymes having been carried out to date.

The five marine fungal isolates characterised in this study were isolated from sediments sampled from Porcupine Bank, at the edge of the West European Continental Shelf in the North Atlantic Ocean [3], and were identified as strains of *P. chrysogenum*, *E. maritima*, *T. stollii* and *P. antarcticum*.

Emericellopsis sp. from the marine environment is of interest in relation to biomass degradation because they have been shown using DNA sequencing methods to possess a large arsenal of CAZyme (carbohydrate-active enzyme)-encoding genes. For example, the genome of *E. atlantica* which was recently sequenced has been shown to possess a large repertoire of CAZymes [20]. *Emericellopsis* sp. TS7 has also been shown using solid-state fermentation to produce xylanase and CMCase activities functional over wide temperature and pH ranges [7]. However, to date, no secretome from *E. maritima* has been quantitatively characterised for its xylanase and exo-glycoside hydrolase activities.

P. chrysogenum is well established as being an efficient degrader of lignocellulosic biomass [21–25]. However, marine *P. chrysogenum* strains have not been well studied to date for this application. To the best of the authors’ knowledge, no secretome from a marine strain of *P. chrysogenum* has been quantitatively characterised for its xylanase activities during LSF.

Research published relating to *P. antarcticum* has been limited in general and has focused previously on meroterpenoid discovery, molecules that have been shown to have anticancer activities [26,27]. To date, there has been no research carried out on the lignocellulolytic enzymes secreted by a strain of *P. antarcticum*, to the best of the authors’ knowledge.

Strains of *T. stollii* are of interest in relation to biomass degradation. The recently sequenced genome of the terrestrial *T. stollii* strain CLY-6 is reported to encode a large repertoire of glycoside hydrolases, totalling 358 [28]. However, strains of *T. stollii* from extreme environments have not previously been studied, and these may have adaptations

to their harsh environments that could benefit industrial processes, making it worthwhile to study such strains.

This work, therefore, aims to profile in detail the lignocellulolytic capabilities of selected fungi from the deep sea, including xylanase, cellulase and phenol oxidase/peroxidase activities. Here, we report the induction and characterisation of an array of lignocellulolytic enzymes secreted by marine fungi isolated from deep-sea sediments in the Atlantic Ocean, and a comparative novel terrestrial *P. chrysogenum* isolate. Lignocellulolytic enzyme induction was achieved using liquid-state fermentation (LSF) on wheat bran (WB), a cheap agricultural by-product, while the profile of secreted lignocellulolytic enzymes was characterised using biochemical approaches and gel-based proteomics.

2. Materials and Methods

2.1. Fungal Isolates Used

Culturable fungal isolates were isolated and purified from deep-sea sediments 900–2000 metres (m) in depth in the Atlantic Ocean off the northwest Irish coast, and the processes of sample collection, isolation and identification of the fungal isolates from deep-sea sediments were described in the Materials and Methods section from reference [3]. The isolates used in this study from the deep sea were *E. maritima* strains SFI-F16 and SFI-D6 (GenBank accession codes MT535805 and MT535802), *P. chrysogenum* strain SFI-D13 (GenBank accession code MT535821), *P. antarcticum* strain SFI-F25 (GenBank accession code MT535816) and *T. stollii* strain SFI-F17 (GenBank accession code MT535842). The comparative novel lignocellulolytic terrestrial isolate was an in-house isolate of *P. chrysogenum* denoted strain BBW2.

2.2. Cultivation of Fungi and Supernatant Harvesting

The isolates were cultivated as described in [29], with modifications. The isolates were first grown and maintained on either Sabouraud Dextrose agar (Neogen, Lansing, MI, USA, product code NCM2012A) or Malt Extract agar (Neogen, Lansing, MI, USA, product #NCM0093A) supplemented with 3% (*w/v*) marine salts (Tetra). To initiate LSF, three 1 cm³ pieces of mycelia from each agar plate were used to inoculate 250 mL Erlenmeyer flasks containing sterilised 100 mL of 0.5% (*w/v*) mycological peptone (Neogen, Lansing, MI, USA, product #NCM0258), 3% (*w/v*) marine salts and 2% (*w/v*) glucose (GLC) (Sigma, St. Louis, MO, USA, product #G8270) in distilled water (dH₂O). Cultures were grown for 48 h (h) in an Innova 44 Incubator Shaker (New Brunswick Scientific, Edison, NJ, USA) at 25 °C, with shaking at 180 rpm. One mL of each isolate culture was then transferred aseptically to duplicate flasks containing sterilised lignocellulolytic enzyme-inducing medium, which was the same as above but with 2% (*w/v*) WB (Odlums, Portlaoise, Ireland) as the inducer instead of GLC. The induction control flask for each isolate contained 2% (*w/v*) GLC instead of WB. LSF was carried out over 144 h at 25 °C, 180 rpm with samples being harvested at specific time points for further analysis.

Cell-free culture supernatants (crude secretomes) were obtained by centrifugation at 3000 rpm for 2 h, at 4 °C in a Beckman Avanti centrifuge (Beckman Coulter, Brea, CA, USA) equipped with a JS5.3 rotor, to separate the solid (mycelia; cells) and liquid fraction of each sample. The liquid fraction from each sample was then transferred carefully to 500 µL microcentrifuge tubes and stored at −80 °C until further analysis. The solid (mycelial) fractions were also stored at −80 °C.

2.3. Xylanase Activity Measurements

The xylanase activity measurements were carried out as described in [29], with modifications. Isolate supernatants (time points taken during 144 h growth time) were tested for their hydrolytic activity against 1% (*w/v*) rye arabinoxylan (Megazyme, Wicklow, Ireland, product #P-RAXY) at pH 5 and 50 °C. Reducing sugars (RS) released in a 10 min (min) reaction was measured using the dinitrosalicylic acid (DNS) method described in [30]. Activity at pH and temperature values between pH 1.5 and 8.0 and 1 and 60 °C was also

measured. The buffer used was 50 mM citric acid-phosphate; temperature range and growth time point measurements were assayed at pH 5.0. Absorbance values were read at 550 nm. Enzymatic activity was calculated by reference to a xylose standard curve and values were expressed as international units per millilitre of the enzyme ($\text{IU}\cdot\text{mL}^{-1}$; $\mu\text{moles RS}\cdot\text{min}^{-1}\cdot\text{mL}^{-1}$).

2.4. Qualitative Plate-Based Assays for Ligninolytic Enzyme Activity

Polyphenol-Oxidase/Peroxidase-like Activity

The isolates were grown on Lignin-Modifying Enzyme Basal Media (LBM) and tested using the syringaldazine well test [31]. Briefly, for the syringaldazine well test, 0.1% syringaldazine in 95% ethanol was added to each duplicate 5 mm well in the agar to test for laccase activity. A second set of triplicate wells contained 0.1% syringaldazine in 95% ethanol and 0.5% (*w/v*) aqueous H_2O_2 to test for peroxidase activity. Ethanol (95% (*v/v*)) was added to a third set of wells to act as a control. The wells for peroxidase activity were only considered positive if there was no colour change in the laccase well or if the laccase well colour was much weaker.

The isolates were also grown on LBM with 20% (*w/v*) GLC and 1% (*w/v*) aqueous tannic acid [31]. This was used to test for general polyphenol oxidase activity, which would show a brown oxidation zone around fungal colonies.

2.5. Exo-Glycoside Hydrolase and Feruloyl Esterase Activity Measurements

The exo-glycoside hydrolase and feruloyl esterase activity measurements were carried out as described in [29], with modifications. Exo-glycoside hydrolase activity measurements were carried out using 4-nitrophenyl (NP)-glycoside substrates, while feruloyl esterase activity was assayed with 4-NP-trans ferulate (Carbosynth, Compton, Berkshire, UK). The detection of hydrolytic activity was based on the release of 4-nitrophenol from the 4-NP substrate. Activity was calculated by reference to a 0.2 mM 4-nitrophenol standard and was expressed in $\text{IU}\cdot\text{mL}^{-1}$ ($\mu\text{moles 4-NP released}\cdot\text{min}^{-1}\cdot\text{mL}^{-1}$). The substrates used were 4-NP- α -L-arabinofuranoside, 4-NP- β -D-cellobioside, 4-NP- α -L-fucopyranoside, 4-NP- β -D-galactopyranoside, 4-NP- β -D-glucopyranoside, 4-NP- β -D-lactopyranoside, 4-NP- β -D-mannopyranoside, 4-NP- α -L-rhamnopyranoside, 4-NP- β -D-xylopyranoside and 4-NP-trans-ferulate. The activities assayed were α -L-arabinofuranosidase, β -xylosidase, cellobiohydrolase (with 4-NP- β -cellobioside and 4-NP- β -lactopyranoside as substrates), β -glucosidase, β -galactosidase, α -rhamnosidase, β -mannosidase, α -fucosidase and feruloyl esterase.

Exo-glycosidase assays were carried out as follows: 10 μL of suitably diluted sample supernatant was added to a 96-well microplate in triplicate. The plate was covered and incubated at 50 °C for 2 min before the addition of 100 μL of 1 mM 4-NP-glycoside, in 50 mM citric acid phosphate buffer, pH 5.0, to test and substrate blank (no enzyme) wells. The reaction mixture was incubated at 50 °C for 10 min. Then, 100 μL of 1 M Na_2CO_3 was added to stop the reaction and develop the colour of enzymatically released 4-NP at alkaline pH. This assay produced a strong yellow colour when there was enzymatic activity; absorbance was read at 410 nm using a microspectrophotometer (BioTek PowerWave XS2, Winooski, VT, USA). There were two modifications to this protocol in relation to two assays: (a) to measure cellobiohydrolase activity and inhibit β -D-glucosidase activity, glucono-1,4- δ -lactone (Sigma, St. Louis, MO, USA, #G4750) was added to assays with 4-NP-cellobioside and 4-NP-lactoside substrates 2 min before assaying for activity, and (b) as 1 M Na_2CO_3 (and NaOH) resulted in saponification (hydrolysis) of the ester link in the 4-NP-trans-ferulate substrate, 1 M Tris-HCl, pH 8.5 was used to as the stopping reagent instead. Activity was quantified by reference to a 0.0–0.2 mM 4-nitrophenol standard curve and the values were converted to $\text{IU}\cdot\text{mL}^{-1}$ of enzyme activity.

2.6. Electrophoresis and Zymography

Semi-denaturing SDS-PAGE was carried out using 8% and 10% polyacrylamide gels with 0.1% (*w/v*) birchwood xylan (Sigma, St. Louis, MO, USA) to test for proteins with xylanolytic activity. The protocol used was a modification of methods from [7,32,33]. Next, 5 to 20 µg of protein (not boiled and no addition of 2-mercaptoethanol) were added to each well of the gel. PageRuler ladders (Thermo Fisher Scientific, Waltham, MA, USA, product codes 11802134, 11852124 and 11892124) were used as molecular weight markers. A commercial Bioglucanase™ enzyme cocktail (Kerry Group, Tralee, Ireland) with xylanolytic activity was used as the positive control. The negative control contained a running buffer only. The gel contained no SDS, but the running buffer and tank buffer contained 0.05% SDS. The gel was run at 200 V for approximately (approx.) 30 min.

After electrophoresis, the gel was washed twice for 15 min with 50 mM sodium citrate buffer, pH 5.0, containing 2.5% (*v/v*) Triton-X-100 or Tween-20 to remove the SDS from the gel (Triton-X-100 was used for *P. antarcticum* zymograms; Tween-20 was used in all other zymogram renaturation procedures). Both are mild non-ionic detergents that carry out the function of removing SDS from proteins and have been used for this purpose in zymography in the work of others [7,32,34]. The gel was then washed twice more for 15 min (per wash) in 50 mM sodium citrate buffer, pH 5.0, to renature the proteins. The gel was then incubated at 50 °C for one hour to allow the reaction to occur. Following this incubation period, the gel was stained with 0.1% (*w/v*) Congo Red (Sigma) solution containing 5% (*v/v*) ethanol for 15 min. The gel was then washed multiple times with 1 M NaCl until clear hydrolysis zones appeared as bands on the gel against a red background. In some cases, the gel was immersed in 1 M HCl for improved contrast of the bands against the background. Gels were illuminated on a visible light box and images were captured using a 25 MP camera (Tristar Electronics, Yeongtong-gu, Suwon, Republic of Korea).

Zymography to test for β-D-xylosidase-active proteins was carried out by running the semi-denaturing SDS-PAGE same as above, without the addition of xylan to the gel. The same washing/renaturing method detailed above was used, along with the same controls. The quantity of protein loaded per well was 40 µg. After electrophoresis, the gels were washed with 50 mM sodium citrate buffer with and without Triton-X-100 or Tween-20 same as described above. The gels were then incubated at 4 °C with 1 mM 4-methylumbelliferyl-β-xylopyranoside (4MUX) (Carbosynth, Compton, Berkshire, UK) in 50 mM sodium citrate buffer, pH 5.0, for 30 min. The gels were then incubated at 50 °C for a further 30 min. Gel images were captured at UV302 using the Azure c300 gel imaging system.

A replica gel was run, in parallel with gels stained for β-xylosidase-active proteins and stained for protein using the Pierce Silver Stain Kit (Thermo Scientific, Waltham, MA, USA, product no. 24612). Gels were imaged using the Azure c300 gel imaging system and used to estimate the size of enzyme-active protein bands.

2.7. Statistics

Statistical analysis of the data was carried out using the arithmetic mean, standard deviation, Student's *t*-test and one-way ANOVA. Analysis was carried out using Microsoft Excel 2016 (Microsoft, Washington, DC, USA). Detailed statistical analysis is available in Supplementary File S1.

3. Results and Discussion

3.1. Xylanase Induction by WB during LSF, and the Qualitative Assessment of Lignin-Degrading Activities

Xylanases play a key role in the degradation of hemicellulose in plant cell walls [35]. Therefore, the isolates in this study were grown on WB during LSF as an inducer of xylanolytic enzyme secretion. WB has been shown in many studies to be a suitable inducer of xylanase production by fungi [29,36–39]. During LSF, enzyme synthesis is repressed and de-repressed/induced by the presence or absence of certain repressors [40]. In the case of xylanase, the repression and de-repression/induction may occur in response to glucose,

xylose and xylan levels in the culture medium [41–43]. Also, secreted enzymes can undergo hydrolysis or degradation during the fermentation process [44]. Therefore, the xylanase activities recorded in the secretome may peak and drop over time.

Xylanase activity against rye arabinoxylan was assessed over a 144 h growth period for each isolate in this study in order to establish the effect of time on xylanase production during the LSF process. Each isolate was also grown on GLC as the carbon source, as a basal carbon source and as induction control. Production of activity on GLC would provide evidence for constitutive activity (and/or derepression of activity later in the growth period when GLC was depleted in the medium). For statistical calculations, refer to Supplementary File S1.

From Figure 1A,B, it is clear that WB induced xylanase production by both strains of *E. maritima*. The highest xylanase activity was recorded at 108 h for SFI-F16 and at 96 h for SFI-D6, with $45 \pm 2.34 \text{ IU}\cdot\text{mL}^{-1}$ and $51 \pm 0.37 \text{ IU}\cdot\text{mL}^{-1}$ of xylanase activity detected in the respective cell-free culture supernatants. These activities were 10.7- and 10.9-fold higher than xylanase present in the secretomes produced on the GLC control for each isolate, respectively. Not only were the peak activities similar between isolates ($p > 0.05$), but the pattern of xylanase activity over time between the two isolates was also similar. Firstly, there was a sharp increase in activity from the 48 h time point until the activity had its first peak at 84 h or 96 h, depending on the strain, followed by a drop in activity 12 h later and the production of a second peak in activity at 108 h or 120 h. The final peak was broad and relatively stable until 132 h but decreased noticeably by the 144 h time point.

To the authors' best knowledge, this is the first time quantitative analysis of xylanase activity has been reported by the *E. maritima* species. To date, only two studies have reported quantitative values for xylanase activity produced by *Emericellopsis* sp. isolates in general. *Emericellopsis* sp. MM FP1.2, isolated from a saline lake in Romania, was reported to produce $5.2 \text{ IU}\cdot\text{mL}^{-1}$ xylanase activity after 5 days LSF on xylan-containing medium [21]. Marine *Emericellopsis* sp. TS11 produced $26.63 \text{ IU}\cdot\text{mg}^{-1}$ protein when tested against oat xylan after LSF for 9 days on xylan-containing medium [7]. This is in comparison to the $7.3 \text{ IU}\cdot\text{mg}^{-1}$ and $50.5 \text{ IU}\cdot\text{mg}^{-1}$ protein produced by *E. maritima* SFI-F16 and SFI-D6 in this study. The xylanase activity reported by MM FP1.2 was not directly comparable to the activities reported in this study, due to differences in experimental conditions reported.

In relation to the *P. chrysogenum* isolates, it was evident that WB markedly induced xylanase production by both the marine (Figure 1C) and terrestrial isolates (Figure 1D). The peak of activity was recorded for both at the 84 h time point and the respective levels were 152 ± 3.11 and $181 \pm 4.73 \text{ IU}\cdot\text{mL}^{-1}$. This represented a 54- and 79-fold increase in xylanase activity when compared to the activity produced in the GLC control flask for each isolate. In fact, of all six fungal isolates, the two *P. chrysogenum* isolates yielded the highest level of xylanase (against rye arabinoxylan) (Figure 1G), with BBW2 producing significantly higher peak xylanase activity ($p < 0.05$) than SFI-D13. The two *P. chrysogenum* isolates shared a distinct pattern of xylanase activity over the 144 h time period. There was a sharp increase in activity at the 72 h time point observed for both isolates, with peak activity occurring at the 84 h time point. Activity decreased sharply at the 96 h time point, with activity remaining low but stable for the remaining time (a slight increase was noted at 120 h, in both culture secretomes).

Xylanase production by *P. antarcticum* SFI-F25 was also induced by WB, albeit at significantly lower levels ($p < 0.05$) than for the *E. maritima* and *P. chrysogenum* isolates (Figure 1E,G). A total of three peaks of xylanase activity were observed in the *P. antarcticum* WB timecourse growth profile, with the highest activity detected at the 96 h time point ($20.5 \pm 2.68 \text{ IU}\cdot\text{mL}^{-1}$), which was 8.2-fold higher than levels in the GLC control. The first peak (shoulder of activity) occurred at 48 h, with a second broader and higher peak from 84–108 h (highest at 96 h) and the third peak at 132 h, after a sharp drop in activity between 108 and 120 h. The third peak was similar in amplitude ($p > 0.05$) to the highest activity peak ($18.12 \pm 0.99 \text{ IU}\cdot\text{mL}^{-1}$). Interestingly, the pattern of activity produced bore no resemblance to the *P. chrysogenum* isolates' activity patterns.

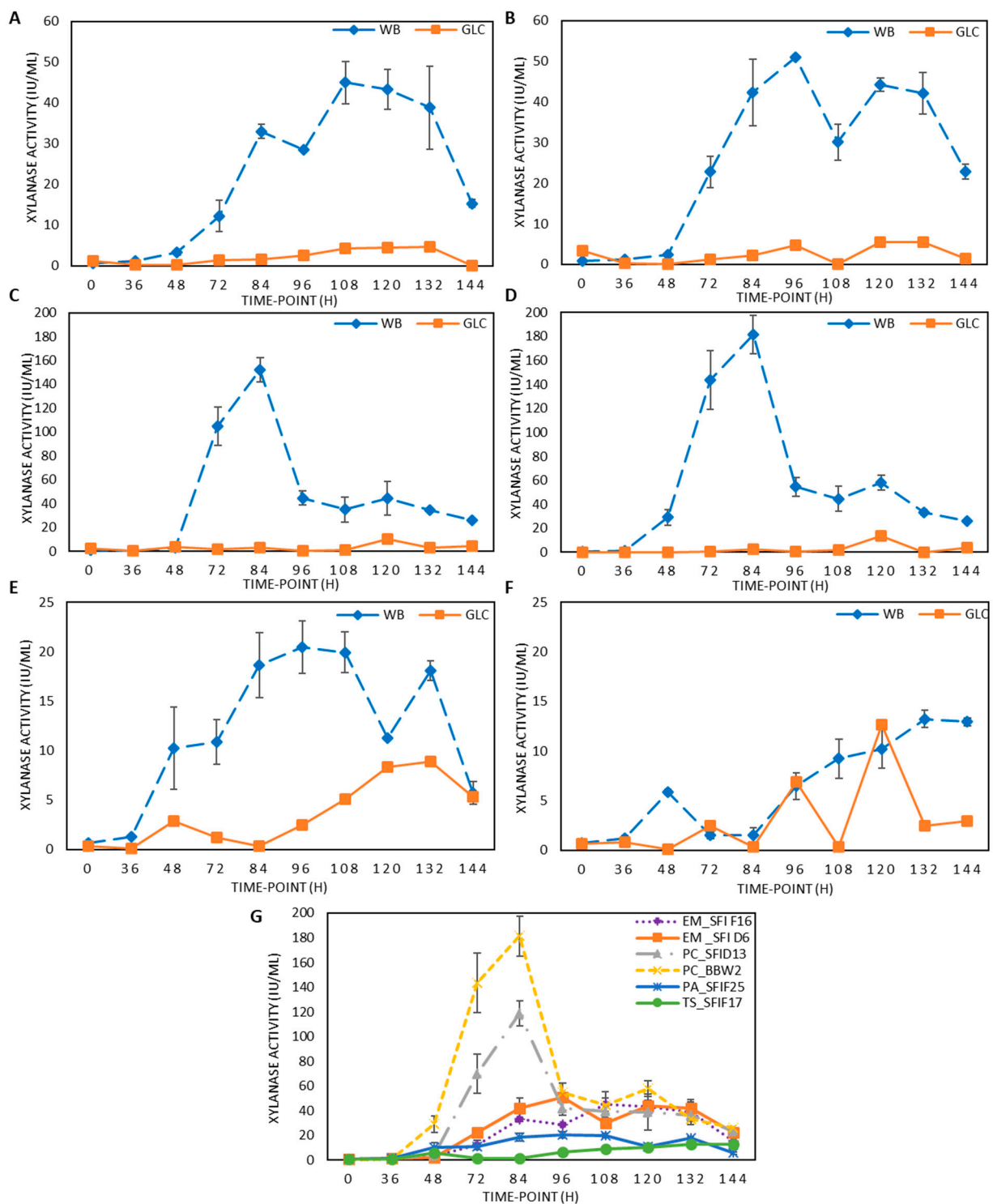


Figure 1. Effect of time point on (A) *E. maritima* SFI-F16; (B) *E. maritima* SFI-D6; (C) *P. chrysogenum* SFI-D13; (D) *P. chrysogenum* BBW2; (E) *P. antarcticum* SFI-F25; and (F) *T. stollii* SFI-F17 xylanase volumetric activity ($\text{IU}\cdot\text{mL}^{-1}$) against rye arabinoxylan at 50 °C and pH 5. (G) Comparison of the effect of time on xylanase volumetric activities ($\text{IU}\cdot\text{mL}^{-1}$) between isolates on WB against rye arabinoxylan at 50 °C and pH 5. EM_SFI16 = *E. maritima* SFI-F16; *E. maritima* SFI-D6 = EM_SFI-D6; *P. chrysogenum* SFI-D13—PC_SFI-D13; *P. chrysogenum* BBW2 = PC_BBW2; *P. antarcticum* SFI-F25 = PA_SFI-F25; *T. stollii* SFI-F17 = TS_SFI-F17. Samples tested were harvested during LSF on WB and GLC substrates at 25 °C and 180 RPM. Error bars represent standard deviation of measurements from duplicate flasks. Statistical differences between samples and isolates are available in Supplementary File S1.

To the authors' best knowledge, prior to this study, no quantitative data on xylanase activity from *P. antarcticum* has been published. However, there have been numerous studies reporting the xylanase activities of *Penicillium* isolates after LSF on different substrates. A study of the terrestrial *P. chrysogenum* PCL501 reported a xylanase production pattern over time during LSF on a WB-containing medium similar to both *P. chrysogenum* isolates in this study. However, the peak activity of $6.47 \text{ IU}\cdot\text{mL}^{-1}$ at the 96 h time point was lower than for the *Penicillium* isolates reported here [45]. A study on a terrestrial *P. sclerotiorum* strain showed this species produced a peak ($13.82 \text{ IU}\cdot\text{mL}^{-1}$) of xylanase activity (against birchwood xylan) after 84 h during LSF on a xylan-containing medium, while terrestrial *Penicillium* sp. SS1 yielded peak xylanase activity ($43.84 \text{ IU}\cdot\text{mL}^{-1}$) after 96 h LSF in a WB-containing medium [46]. Overall, peak xylanase production by both of the *Penicillium* isolates in these latter studies occurred around the 84–96 h growth time point, similar to the *P. chrysogenum* isolates from this study.

To the best of the authors' knowledge, this study is the first to quantitatively characterise the xylanase activity ($\text{IU}\cdot\text{mL}^{-1}$) secreted by a marine *P. chrysogenum* during LSF [47]. Prior to this study, only marine *P. chrysogenum* FS010 had been studied for its xylanase activity. The study recorded xylanase activity produced by *P. chrysogenum* FS010 by measuring the diameters of hydrolytic halos on minimum medium agar with 0.5% (*w/v*) xylan. The xylanase enzyme was also overexpressed in *E. coli* BL21, with specific xylanase activity measured at $10,210 \text{ U}\cdot\text{mg}^{-1}$ against birchwood xylan.

T. stollii SFI-F17 also produced xylanase at significantly lower peak levels than *E. maritima* and *P. chrysogenum* isolates ($p < 0.05$), but at similar peak levels as *P. antarcticum* SFI-F25 ($p > 0.05$). An initial peak of xylanase was produced at 48 h ($5.8 \text{ IU}\cdot\text{mL}^{-1}$) on WB, followed by a drop in activity levels by 72 h. Xylanase production increased from 84 h onwards reaching a maximum at 132 h ($13.2 \pm 0.88 \text{ IU}\cdot\text{mL}^{-1}$). When grown on GLC, growing peaks in xylanase activity were also observed over time. This suggested that *T. stollii* SFI-F17 produced xylanase constitutively, and also suggested derepression of xylanase production, as higher activity was produced after 72 h when GLC levels are likely to be depleted in the medium. Overall, it was concluded that WB improved xylanase production by *T. stollii* SFI-F17, by making levels more consistent over time in contrast to growth on GLC.

To the best of the authors' knowledge, this study is the first to characterise xylanase activity by a marine isolate of *T. stollii*. Many studies have been conducted on the xylanase activity of *Talaromyces* sp. isolates. A terrestrial *T. amestolkiae* was recently reported to produce $13.02 \text{ IU}\cdot\text{mL}^{-1}$ xylanase activity against larchwood xylan after a 168 h LSF on a WB-containing medium [39]. This was similar to the activity produced by the *T. stollii* isolate in this study after 132 h of LSF. A study of terrestrial *T. stollii* LV186 showed that 5 days of LSF on a GLC and corn stover-containing medium yielded xylanase activity of approx. $7.5 \text{ IU}\cdot\text{mL}^{-1}$, with this activity remaining stable for the remaining ten days of the experiment [48]. The increase in activity and stability from day 5 onwards in the aforementioned study was similar to the activity pattern observed in this study.

In general, it was challenging to directly compare activity values between studies due to methodology variations. However, in the aforementioned studies on *Talaromyces* sp. xylanase activity, the production patterns were similar between all, even though the culture conditions varied. Therefore, xylanase activity profiles over time during LSF on WB-containing medium may be quite predictable, even with variations in culture conditions, for some closely related strains of the *Talaromyces* sp.

To screen for lignin-degrading activities, all isolates were tested qualitatively using a plate-based assay for polyphenol oxidase/peroxidase-like activities. However, none of the isolates showed this type of activity.

Some *Emercellopsis* sp. have been shown to produce polyphenol oxidase activity, while others have been shown to not produce this type of activity. *E. maritima* CBS 491.71, as well as five other *Emercellopsis* isolates, were shown to not possess polyphenol oxidase activity, while the remaining nine *Emercellopsis* isolates studied had polyphenol oxidase activity [49].

There were reports of peroxidase/polyphenol oxidase activities by some *P. chrysogenum* isolates, while no peroxidase/polyphenol oxidase activities were reported for others [50,51]. To the authors' best knowledge, there have been no reports on these activities from *P. antarcticum*. *T. stollii* was previously reported to produce laccase activity [51], while no other polyphenol oxidase/peroxidase activities have so far been recorded for this species.

Overall, it is suggested that polyphenol oxidase/peroxidase activities as reported across these studies are highly strain-specific, rather than species-specific.

3.2. Exo-Acting Glycoside Hydrolase and Feruloyl Esterase Induction by WB during LSF

After LSF on WB and GLC, the isolate supernatant samples were screened quantitatively for a variety of exo-acting glycoside hydrolase activities and feruloyl esterase. Specifically, production of α -L-arabinofuranosidase, β -D-xylosidase, β -D-glucosidase, cellobiohydrolase (against β -D-cellobioside and β -D-lactoside), β -D-mannosidase, α -L-fucosidase, α -L-rhamnosidase and β -D-galactosidase activities were investigated. These enzymes are important in the degradation of lignocellulosic biomass, and fungi producing these in abundance may be useful for bioconversion of biomass prior to biofuel production. Figure 2 demonstrates the relative levels of these enzymes produced by each isolate during LSF on WB and GLC for 144 h. For statistical calculations, refer to Supplementary File S1.

Figure 2A,B shows that both *E. maritima* strains secreted all of the tested enzymes. It was evident that WB induced greater levels of the enzymes assessed compared to GLC, except for β -D-galactosidase and β -D-mannosidase, where there was no notable difference between WB and GLC secretomes.

For *E. maritima* SFI-F16, β -D-glucosidase activity increased until 120 h and then decreased slightly at the 132 h and 144 h time points. For *E. maritima* SFI-D6, β -D-glucosidase activity continuously increased over the time period assessed. SFI-D6 produced similar peak β -D-glucosidase activities (1.33 ± 0.05 IU·mL⁻¹) to SFI-F16 (1.24 ± 0.12 IU·mL⁻¹) ($p < 0.05$). The β -D-cellobiosidase activity detected in the SFI-F16 secretome was observed from 48 h onwards, with the peak activity occurring at 72 h, and less of this enzyme was produced from 84–144 h. For SFI-D6, β -D-cellobiosidase activity was first detected at 36 h, while from 72–144 h, there was a relatively stable amount of this activity produced. Interestingly, at the peak production point for both isolates, SFI-F16 produced significantly (4.8 fold) more β -D-cellobiosidase than SFI-D6, with SFI-F16 producing 0.56 ± 0.05 IU·mL⁻¹ and SFI-D6 producing 0.12 ± 0.01 IU·mL⁻¹ ($p < 0.05$).

SFI-F16 also produced significantly (3.7-fold) more α -L-arabinofuranosidase than SFI-D6, with SFI-F16 producing 1.4 ± 0.08 IU·mL⁻¹ and SFI-D6 producing 0.38 ± 0.07 IU·mL⁻¹ at their respective optimum activity time points ($p < 0.05$). The most significant difference was noted for the β -D-lactopyranoside activities, with SFI-F16 producing significantly (11.2 fold) more of this activity (0.2 ± 0.03 IU·mL⁻¹) than SFI-D6 (0.03 ± 0.01 IU·mL⁻¹) ($p < 0.05$). Activity against this substrate can represent cellobiohydrolase type 1 activity (GH7) and/or endoglucanase activity.

Feruloyl esterase was produced by SFI-F16 only at the 120 h and 132 h time points, with the highest activity being produced at 132 h. In contrast, SFI-D6 produced feruloyl esterase activity mostly at the 36 h time point, while also producing it at the later (132 h and 144 h) time points. The remaining exo-acting glycoside hydrolase activities were produced by both isolates in very low amounts when compared to the abovementioned activities. Overall, SFI-F16 produced significantly more ($p < 0.05$) β -D-cellobiosidase than the other isolates assessed in this study, except for *T. stollii* SFI-F17 ($p > 0.05$), and significantly more α -L-arabinofuranosidase than all other isolates assessed ($p < 0.05$).

Genomic and metabolomic studies of two marine strains, *E. cladophorae* MUM 19.33 and *E. cladophorae* TS7, showed evidence for the presence of diverse glycoside hydrolases as well as carbohydrate esterase-encoding genes [20,49], while *Emericellopsis* sp. TS11 demonstrated xylanase and CMCase activities [7]. The existence of exo-acting glycoside hydrolase and feruloyl esterase activities in secretomes produced by deep-sea *Emericellopsis*

sp., such as the *E. maritima* strains reported here and *E. cladophorae* TS7, are interesting, as the environment which they were isolated from does not have an abundance of plant biomass/matter, with our oceans containing less than 0.2% of global plant biomass [52]. To the best of the authors' knowledge, this is the first time exo-glycoside hydrolase and feruloyl esterase activities have been reported in *E. maritima*.

In Figure 2C,D, it was observed that both *P. chrysogenum* strains assessed secreted all of the tested accessory enzyme activities. It was evident that WB induced much greater production of the enzymes assessed when compared to GLC, with the exception of β -D-mannosidase, feruloyl esterase and α -L-fucosidase, where there was no significant difference in activity between WB and GLC cultures. In both *P. chrysogenum* isolates, the highest exo-acting glycoside hydrolase activity levels were recorded for β -D-glucosidase, β -D-galactosidase and β -D-xylosidase.

For SFI-D13, β -D-glucosidase activity increased up to the 144 h time point, where it reached $1.54 \pm 0.1 \text{ IU}\cdot\text{mL}^{-1}$. For BBW2, the β -D-glucosidase activity was similar ($p > 0.05$) to that of SFI-D13 and increased until the 132 h time point, where it reached $2.2 \pm 0.01 \text{ IU}\cdot\text{mL}^{-1}$, then decreased by the 144 h time point. The β -D-galactosidase activity for both isolates increased until the 132 h time point, where SFI-D13 produced significantly more (1.9 fold) activity ($0.83 \pm 0.04 \text{ IU}\cdot\text{mL}^{-1}$) than BBW2 ($0.43 \pm 0.01 \text{ IU}\cdot\text{mL}^{-1}$) ($p < 0.05$), with activity decreasing by the 144 h time point. For the β -D-xylosidase, the activity of SFI-D13 and BBW2 increased until the 132 h and 120 h time points, reaching similar peak activities of $0.28 \pm 0.02 \text{ IU}\cdot\text{mL}^{-1}$ and $0.26 \pm 0.005 \text{ IU}\cdot\text{mL}^{-1}$, respectively ($p > 0.05$). Both isolates also produce relatively stable α -L-arabinofuranosidase activities after 48 h, with both isolates' activities peaking at $0.23 \pm 0.02 \text{ IU}\cdot\text{mL}^{-1}$.

The largest difference between the two isolates is between β -D-cellobiosidase activities, which have the highest activities of $0.03 \pm 0.01 \text{ IU}\cdot\text{mL}^{-1}$ and $0.12 \pm 0.01 \text{ IU}\cdot\text{mL}^{-1}$ for SFI-D13 and strain BBW2, respectively. This represents a significant (4 fold) difference in this activity between the isolates ($p < 0.05$). The other exo-acting glycoside hydrolase activities assessed were all present in secretomes from both *P. chrysogenum* isolates, but in much smaller amounts than the activities detailed above. Overall, both *P. chrysogenum* exo-acting glycoside hydrolase profiles are remarkably similar. BBW2 also produced the most α -L-rhamnosidase activity out of all isolates studied ($p < 0.05$).

In Figure 2E, the exo-acting glycoside hydrolase and feruloyl esterase activities secreted by *P. antarcticum* SFI-F25 are presented. All enzyme activities assessed were induced by WB, except for α -L-rhamnosidase and feruloyl esterase activities, where there was no significant difference in activity noted between WB and GLC secretomes.

In contrast to the other isolates, the main activity produced by this isolate between 48–144 h was β -D-xylosidase, with the highest activity of $0.44 \pm 0.01 \text{ IU}\cdot\text{mL}^{-1}$ at 144 h. This was followed by α -L-arabinofuranosidase, β -D-glucosidase and β -D-galactosidase which also peaked at the 144 h time point with activity levels of $0.21 \pm 0.001 \text{ IU}\cdot\text{mL}^{-1}$, $0.18 \pm 0.001 \text{ IU}\cdot\text{mL}^{-1}$ and $0.13 \pm 0.005 \text{ IU}\cdot\text{mL}^{-1}$, respectively. Notably, there was a large induction of β -D-mannosidase at 132 h of $0.33 \text{ IU}\cdot\text{mL}^{-1}$, making this isolate the best producer of β -D-mannosidase activity when compared to all of the other isolates investigated in this study ($p < 0.05$). However, under the assay conditions used, it has the lowest combined exo-glycosidic activity (maximum combined total of $1 \text{ IU}\cdot\text{mL}^{-1}$) when compared to the other isolates. To the best of the authors' knowledge, this is the first time that exo-glycoside hydrolase and feruloyl esterase activities have been reported in *P. antarcticum*.

T.stollii SFI-F17 secreted all of the tested enzyme activities (Figure 2F). WB induced greater production of all of the enzymes assessed when compared to GLC. The highest exo-acting glycoside hydrolase activities for this isolate were recorded for β -D-galactosidase, β -D-glucosidase, β -D-xylosidase, α -L-arabinofuranosidase and β -D-lactopyranosidase. The average activities for these enzymes at their peak production time points on WB were $2.3 \pm 0.09 \text{ IU}\cdot\text{mL}^{-1}$, $2.3 \pm 0.23 \text{ IU}\cdot\text{mL}^{-1}$, $1.38 \pm 0.08 \text{ IU}\cdot\text{mL}^{-1}$, $0.76 \pm 0.05 \text{ IU}\cdot\text{mL}^{-1}$ and $0.63 \pm 0.07 \text{ IU}\cdot\text{mL}^{-1}$, respectively. β -D-Cellobiosidase activity was reported as $0.26 \pm 0.02 \text{ IU}\cdot\text{mL}^{-1}$.

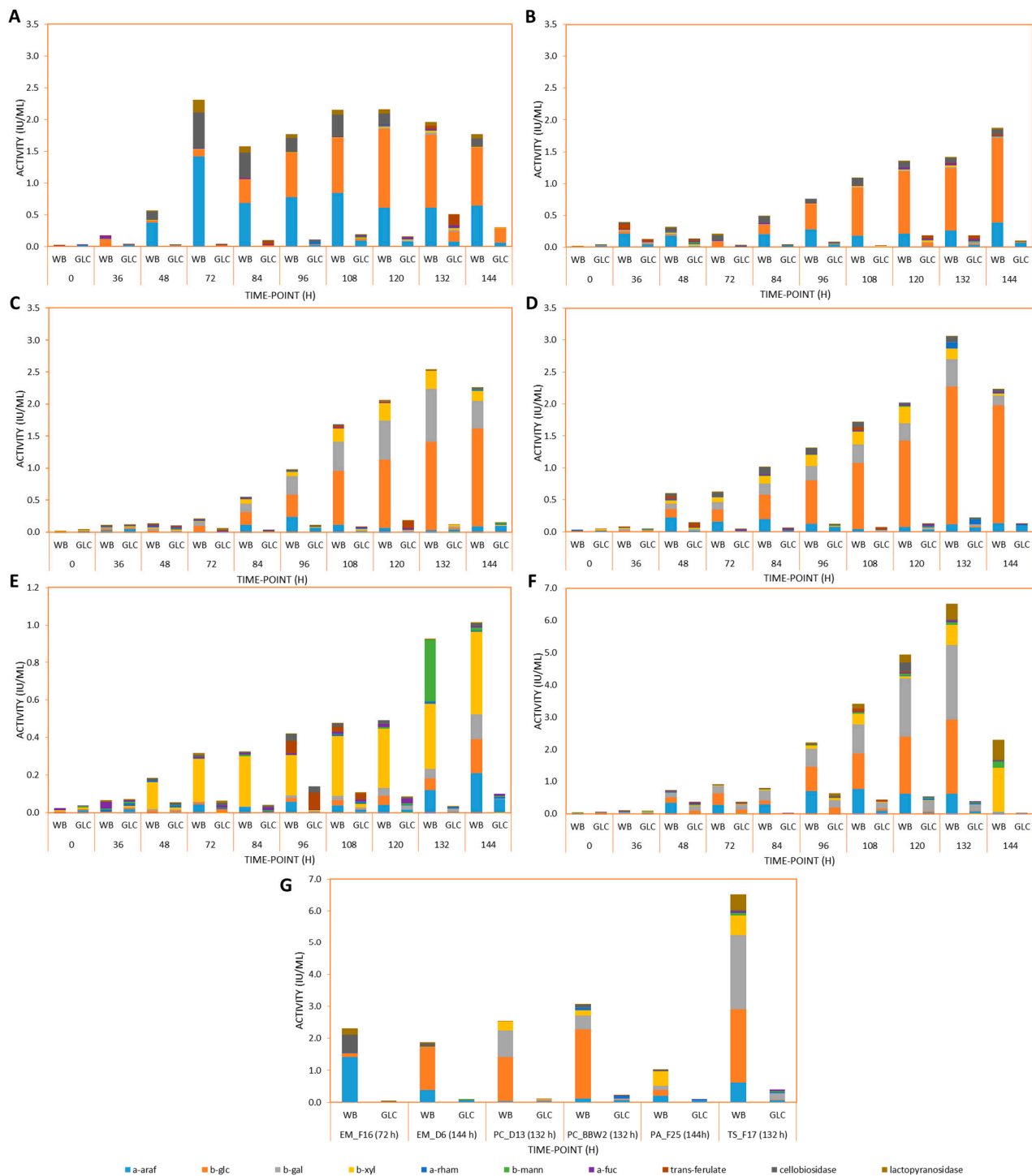


Figure 2. Relative levels of exo-acting glycoside hydrolases and feruloyl esterase (IU·mL⁻¹) produced by (A) *E. maritima* SFI-F16; (B) *E. maritima* SFI-D6; (C) *P. chrysogenum* SFI-D13; (D) *P. chrysogenum* BBW2; (E) *P. antarcticum* SFI-F25; and (F) *T. stollii* SFI-F17. (G) shows the time points with the highest cumulative exo-enzyme production for each isolate at the same scale. Activities shown are for α -L-arabinofuranosidase (a-araf), β -D-xylosidase (b-xyl), β -D-glucosidase (b-glc), cellobiohydrolase (against β -D-cellobioside (cellobiosidase) and β -D-lactoside (lactopyranosidase)), β -D-mannosidase (b-mann), α -L-fucosidase (a-fuc), α -L-rhamnosidase (a-rham), β -D-galactosidase (b-gal) and the carbohydrate esterase feruloyl esterase. WB and GLC denote WB-containing duplicate flasks (mean value) and the GLC-containing flask at each time point. Statistical differences between samples and isolates are available in Supplementary File S1.

Compared to all other isolates in this study, *T. stollii* SFI-F17 produced the most exo-acting glycoside hydrolase activities over the assessed time period on WB, with a combined total of $8.02 \text{ IU}\cdot\text{mL}^{-1}$ at the peak-production time point, across the exo-glycoside hydrolase and feruloyl esterase activities investigated and under the assay conditions used. *E. maritima* SFI-F16 and SFI-D6 produced combined totals of $3.58 \text{ IU}\cdot\text{mL}^{-1}$ and $1.99 \text{ IU}\cdot\text{mL}^{-1}$, while *P. chrysogenum* SFI-D13 and BBW2 produced combined totals of $3.07 \text{ IU}\cdot\text{mL}^{-1}$ and $3.38 \text{ IU}\cdot\text{mL}^{-1}$. For individual activities, *T. stollii* produced the most β -D-galactosidase, β -D-xylosidase and β -D-lactopyranosidase activities when compared to the other isolates studied ($p < 0.05$).

To the best of the authors' knowledge, this study is the first to characterise lignocellulolytic activities in a marine isolate of *T. stollii*. In terms of *T. stollii* in general, this study is the first to report α -L-arabinofuranosidase, β -D-galactosidase, β -D-lactosidase, α -L-fucosidase, β -D-mannosidase and feruloyl esterase activities.

In another study, *T. stollii* LV186 was shown to produce β -D-xylosidase and β -D-glucosidase activities of approx. $2.5 \text{ IU}\cdot\text{mL}^{-1}$ and $0.13 \text{ IU}\cdot\text{mL}^{-1}$ after 5 days of LSF on GLC and corn stover, respectively [48]. A further study observed both α -L-rhamnosidase and β -D-glucosidase activity production by *T. stollii* CLY-6 [28,53]. The closely related *T. amestolkiae* had β -D-glucosidase activity of $1.9 \text{ IU}\cdot\text{mL}^{-1}$ under similar LSF conditions as were used in this study [28]. A remarkably similar activity for cellobiosidase was also reported for *T. amestolkiae* at approx. $0.3 \text{ IU}\cdot\text{mL}^{-1}$ after 5 days of LSF on xylan-containing medium, as well as a lower β -D-glucosidase value of approx. $1 \text{ IU}\cdot\text{mL}^{-1}$ [54]. Furthermore, a substantially lower level of β -D-xylosidase activity of $0.8 \text{ IU}\cdot\text{mL}^{-1}$ was reported for *T. amestolkiae* [55].

Overall, *T. stollii* SFI-F17 produced the largest amount of exo-glycoside hydrolase activities when compared to the *Penicillium* sp. and *E. maritima* isolates studied. This finding was supported by the fact that the sequenced genome of terrestrial *T. stollii* CLY-6 was reported to encode 358 glycoside hydrolases [28], while *P. rubens* (also known as *P. chrysogenum*) was reported to encode 222 CAZymes (CAZy database) and *Emericellopsis* sp. TS7 was reported to encode 217 CAZymes [20].

Furthermore, a terrestrial strain of *T. stollii* was shown to produce crude enzymes that degraded over 30% of cellulose to glucose in sorghum and corn stover agri-wastes, while the commercial cocktail Celluclast, containing enzymes from the industrial workhorse *Trichoderma reesei* degraded less than 20% of cellulose to glucose on the same agri-wastes [48]. Therefore, it is possible that enzyme cocktails from strains of *T. stollii*, such as those reported in this study and in [48], could eventually be adapted for commercial use.

3.3. Effect of Temperature and pH on Xylanase Activity in the Fungal Secretomes

Fungal xylanases usually have a pH optima of between 4 and 6 [7,23,39,56,57]. Therefore, the measurement of temperature optima for each isolate was carried out at pH 5. The profile of secreted xylanase activity for each isolate at temperatures between 1–60 °C is represented in Figure S1 (Supplementary File S2). For statistical calculations, also refer to Supplementary File S1.

E. maritima isolate xylanase activities showed very different responses over the temperature range assessed when compared with each other. Xylanase from *E. maritima* SFI-F16 showed 87.6% and 90.7% of its maximum activity at 30 °C and 40 °C, and 55.9% at 60 °C, with optimal activity at 50 °C (Supplementary File S2, Figure S1A). The xylanase activity at 30 °C, 40 °C and 50 °C were not significantly different ($p > 0.05$), indicating the stability of the xylanase activity in this temperature range.

E. maritima SFI-D6, on the other hand, exhibited 34.3% of its optimal xylanase activity at 20 °C, 68.7% at 30 °C and 32.4% at 50 °C, with its optimal xylanase activity at 40 °C (Supplementary File S2, Figure S1B), which indicated a narrower range of near-optimal xylanase activity for xylanase from *E. maritima* SFI-D6 than SFI-F16. While there was no significant difference in activity at 30 °C and 40 °C ($p > 0.05$), there was a significant difference in activity between 40 °C and 50 °C ($p < 0.05$). Marine *Emericellopsis* sp. strain

TS11 also produced xylanase with optimum activity at 50 °C, similar to *E. maritima* strain SFI-F16 in this study [7].

Marine *P. chrysogenum* SFI-D13 showed relative xylanase activities of 12.2% and 31.6% at 1 °C and 10 °C (Supplementary File S2, Figure S1C), while terrestrial BBW2 had xylanase activity, relative to the optimum, of 7.9% and 19.9% at 1 °C and 10 °C (Supplementary File S2, Figure S1D), with optimum xylanase activity recorded at 40 °C for both isolates. While the *P. chrysogenum* isolates had similar relative activities at 20 °C and 30 °C ($p > 0.05$), SFI-D13 retained 80.2% of its optimum xylanase activity at 50 °C, while BBW2 only retained 31.4% of its optimum at this temperature. Overall, the marine *P. chrysogenum* had xylanase activity that did not vary significantly between 1–10 °C, 10–20 °C and 40–50 °C ($p > 0.05$), while it varied significantly at each temperature tested for the terrestrial isolate ($p < 0.05$). Temperature optima for other *P. chrysogenum* and *Penicillium* sp. isolates have also been reported at 40 °C [24,58].

The *P. antarcticum* isolate xylanase retained activity relative to the optimum of at least 25.7% at all temperatures assessed (Supplementary File S2, Figure S1E), while the *T. stollii* isolate xylanase retained a relative activity of at least 35.6% at all temperatures (Supplementary File S2, Figure S1F). For both isolates, there was no statistically significant difference in xylanase activity between 1–10 °C, 1–20 °C, 10–20 °C, 20–30 °C and 50–60 °C ($p > 0.05$). A similarly wide xylanase activity range between temperatures of 30–80 °C was reported for *T. amestolkiae* [39].

For all isolates, except for *E. maritima* SFI-F16 which had a temperature optimum for xylanase activity of 50 °C, the temperature optimum for secreted xylanase was 40 °C. Additionally, all isolates produced cold-active xylanases that had at least some activity at each of the temperatures tested, indicating a wide range of temperature functionality amongst the isolates. The terrestrial *P. chrysogenum* BBW2 crude xylanase activity appeared to have the poorest versatility over the assessed temperature range, with significant differences in activity between temperatures ($p < 0.05$), while xylanase activities produced by *P. antarcticum* SFI-F25, *T. stollii* SFI-F17 and *E. maritima* SFI-F16 appeared to be the most versatile, with their xylanase activities not varying significantly over a wide temperature range.

The pH optimum for each isolate xylanase activity was determined over a pH range of 3.0–8.0 (Supplementary File S2, Figure S2), while the activity for *T. stollii* was also determined at pH 1.5, 2.0 and 3.5 due to its acidophilic nature (Supplementary File S2, Figure S2F). The pH measurements were carried out at 50 °C, as the optimal temperature for fungal xylanases, apart from enzymes from thermotolerant and thermophilic species, is usually between 40–60 °C [59].

The pH optimum for xylanase activity from *E. maritima* SFI-F16 (Supplementary File S2, Figure S2A) was pH 6.0. Crude xylanase from this source retained 55% of its optimum xylanase activity at pH 5.0, 66% at pH 7.0 and 31.2% at pH 8.0, showing a wide pH range of functionality for the xylanases from this isolate. However, this isolate did not produce any xylanase active at pH 3.0, and only 5% of the optimum activity was present at pH 4.0.

In relation to xylanase activity from *E. maritima* SFI-D6 (Supplementary File S2, Figure S2B), the pH optimum for xylanase activity was pH 5.0. Unlike *E. maritima* SFI-F16, xylanase activity from this isolate did not have high activity relative to the optimum across the pH range assessed, and the differences in activities between the optimum and all other pH values assayed varied significantly ($p < 0.05$). The crude xylanase displayed 36.2% and 36.6% of its optimum xylanase activity at pH 6.0 and 7.0, while xylanase activity was not detected at pH 3.0, 4.0 and 8.0, respectively.

In a different study, crude xylanase from *Emericellopsis* sp. was found to have a profile of activity over a range of pH values similar to that of *E. maritima* SFI-F16 reported in this study. This isolate also had a xylanase activity pH optimum of pH 6.0, while retaining activity between pH 4.0 and 10.0. This could potentially reflect an adaptation by these fungal isolates to the pH range present in their natural environment, the Atlantic Ocean, the waters of which are currently pH 8.1 [19,60].

The two *P. chrysogenum* isolates studied had quite different xylanase activity profiles over the pH range assessed, similar to the two *E. maritima* isolates. *P. chrysogenum* SFI-D13 (Supplementary File S2, Figure S2C) showed a versatile xylanase activity profile, with activity between pH 4.0 and 7.0. The optimum xylanase activity was observed at pH 5.0. The relative xylanase activities at pH 4.0, 6.0, and 7.0 were 80.5%, 95.2% and 36.5% of the optimum, with activity at pH 3.0 and 8.0 being 8.4% and 5.3% of the optimum. The activities at pH 5.0 and 6.0 did not vary significantly ($p > 0.05$), demonstrating xylanase activity stability at these pH values.

P. chrysogenum BBW2 was less versatile than SFI-D13. The optimum pH for xylanase activity was at pH 6.0. The activities recorded at pH 4.0, 5.0 and 7.0 were 31%, 42.2% and 39% of the optimum, respectively. Furthermore, the xylanase activities recorded at pH 3.0 and 8.0 were 9.8% and 3.6% of the optimum. The xylanase activity varied significantly between each pH value measured ($p < 0.05$), indicating that the xylanase activity in this case was unstable except at pH 6.0. In other studies, the pH optima for crude xylanases from *P. chrysogenum* were reported to be pH 5.0 and 6.0 [23–25].

P. antarcticum SFI-F25 (Supplementary File S2, Figure S2E) produced xylanase that had optimal activity at pH 5.0. It also had activity that was functional between pH 3.0 and 7.0, but not at pH 8.0. Xylanase activity at pH 3.0, 4.0, 6.0 and 7.0 were 28.6%, 30.7%, 49.8% and 31.8% of the optimum activity. Activities at pH 4.0 and 6.0 also varied significantly from that at pH 5.0 ($p < 0.05$), indicating that the xylanase activity produced by SFI-F25 became relatively unstable when not at the optimum pH.

T. stollii SFI-F17 (Supplementary File S2, Figure S2F) produced acidophilic xylanase activity, which functioned optimally at pH 3.5 and retained 6.8%, 56.4%, 61.6%, 88.8%, 49.9%, 13.2%, 6.6% and 2.4% of its optimal activity at pH 1.5, 2.0, 3.0, 4.0, 5.0, 6.0, 7.0 and 8.0. Between pH 2.0–3.0 and 3.0–4.0, there was no significant difference in activity ($p > 0.05$), indicating xylanase activity was stable at these pH values.

A similar xylanase activity profile from pH 3.0–8.0 was reported for *T. amestolkiae*, which had a pH optimum of 4.0 and activity gradually decreased to its lowest activity at pH 8.0 [39]. A different study of *T. amestolkiae* showed maximal activity for its xylanase at pH 3.0 that gradually decreased as pH increased, similar to observations for the *T. stollii* crude xylanase activity reported in this study [55]. Acidophilic xylanases may be useful in the production of bioethanol [61], for example as part of a combined pre-treatment strategy by pre-treating lignocellulosic biomass with acidophilic xylanases at an acidic pH.

3.4. Electrophoretic Separation of Proteins in the Crude Secretomes and Zymogram Analysis

Electrophoretic separation of proteins in the crude fungal secretomes, under mildly denaturing conditions, was combined with zymograms analysis to investigate the presence and number of enzyme-active bands, to determine the approx. molecular weights of the xylan-degrading enzymes in each WB secretome and to analyse the changes in the xylan-degrading proteins over time. The exo-xylan degrading activity (β -D-xylosidase) was analysed using the fluorescent 4MUX substrate, while xylanase active proteins (endo- β -1,4-D-xylanase) were determined using an in-gel xylan substrate method. Proteins present in the crude 48 h, 96 h and 144 h secretomes were analysed, to represent early, mid and late secretion profiles. Two samples were analysed for each time point, representing each of the duplicate lignocellulolytic-inducing cultures. Specifically in relation to the β -D-xylosidase activity gels for the *E. maritima* isolates, it was difficult to determine the molecular weight of these activity bands when compared to the silver-stained gels, because of the large number of protein bands with similar molecular weights present on the corresponding silver-stained gels (Figure 3A,C). Therefore, the molecular weights of the activity bands from the *E. maritima* β -D-xylosidase gels have been given as rough estimates.

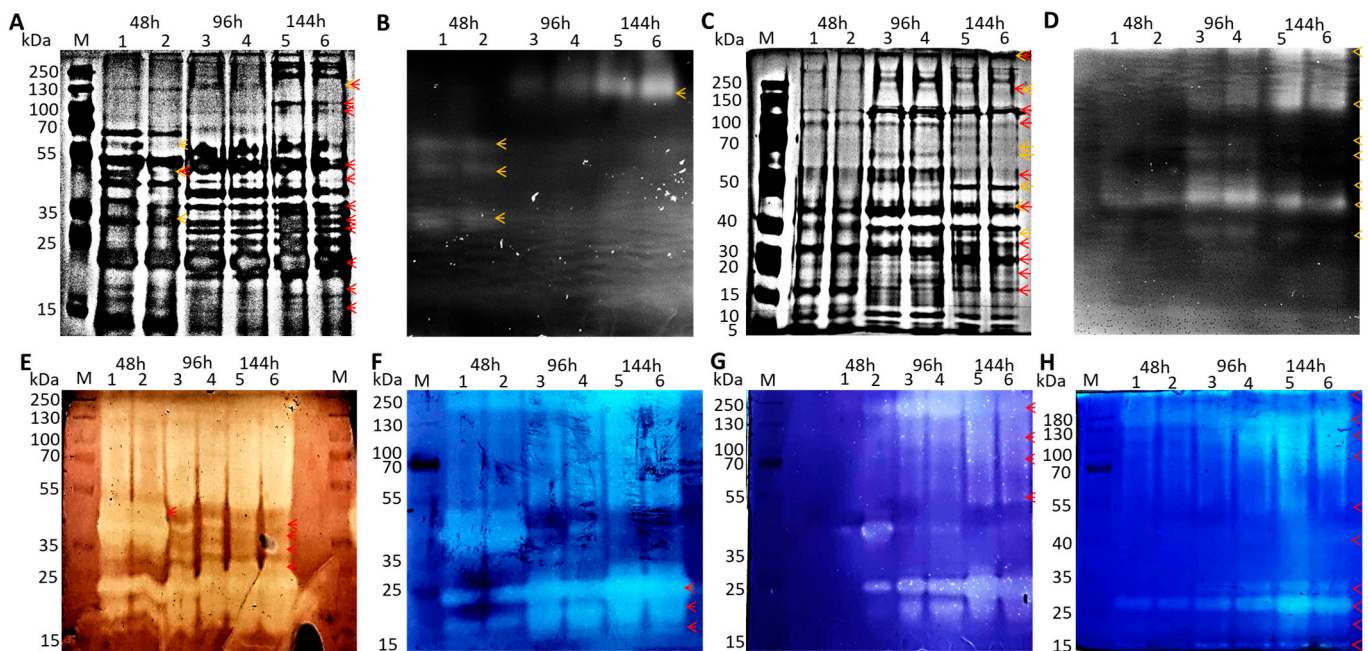


Figure 3. Electrophoretic and zymogram analysis of secretome profiles of *E. maritima* SFI-F16 (A,B,E–G) and SFI-D6 (C,D,H), when grown on WB during LSF, is represented in this figure. (A) and (C) are 8% silver stained gels of the isolate secretomes of strains SFI-F16 (A) and SFI-D6 (C) at the sampled time points (1 and 2 = 48 h; 3 and 4 = 96 h; 5 and 6 = 144 h; M = molecular weight marker), each with 10 μ g of protein loaded/well; (B) and (D) are 8% zymograms of isolate SFI-F16 (B) and SFI-D6 (D) supernatants incubated with the fluorescent 4MUX substrate and 40 μ g of protein/well (1 and 2 = 48 h; 3 and 4 = 96 h; 5 and 6 = 144 h; M = molecular weight marker); (E) is an 8% zymogram of strain SFI-F16 with in-gel xylan substrate and 20 μ g of protein loaded/well (1 and 2 = 48 h; 3 and 4 = 96 h; 5 and 6 = 144 h; M = molecular weight marker); (F) is an 8% zymogram of strain SFI-F16 with in-gel xylan substrate (10 μ g of protein loaded/well), and band enhancement with 1 M HCl (1 and 2 = 48 h; 3 and 4 = 96 h; 5 and 6 = 144 h; M = molecular weight marker); (G) is an 8% zymogram of strain SFI-F16 with in-gel xylan substrate (5 μ g of protein loaded/well), and band enhancement with 1 M HCl (1 and 2 = 48 h; 3 and 4 = 96 h; 5 and 6 = 144 h; M = molecular weight marker). (H) is an 8% zymogram of strain SFI-D6 with in-gel xylan substrate (10 μ g of protein loaded/well), and band enhancement with 1 M HCl (1 and 2 = 48 h; 3 and 4 = 96 h; 5 and 6 = 144 h; M = molecular weight marker). Yellow arrows signify β -D-xylosidase activity bands. Red arrows signify endo- β -D-xylanase activity bands. The approx. locations of the activity bands are also shown in each respective silver-stained gel (A,C). Original images of gels are available in Supplementary File S3.

The xylan-degrading enzyme secretome profiles of *E. maritima* SFI-F16 and SFI-D6 when grown on WB during LSF are presented in Figure 3. When the zymogram testing for β -D-xylosidase activity from SFI-F16 was carried out, three activity bands were observed at approx. 35, 50 and 65 kDa at the 48 h time point when enzyme active bands were compared with the silver-stained protein gel (Figure 3A,B, lanes 1 and 2). At the 96 h and 144 h time points, a band was observed at approx. 160 kDa when compared to the silver-stained gel (Figure 3A,B; lanes 3–6). These results showed that the isolate produced four β -D-xylosidase activity bands. This isolate, therefore, may have favoured the secretion of smaller β -D-xylosidases at the 48 h time point during the LSF on WB, while a larger one may have been secreted at the later time points. However, it has been shown that β -D-xylosidases can have more than one subunit that can exist and function in equilibrium between monomeric and oligomeric forms in solution [62]. So, it may instead be the case that multiple subunits of the same β -D-xylosidase complex are being visualised on the gel.

When zymograms testing for β -D-xylanase activities by SFI-F16 were carried out, twelve xylanase isoforms were observed at approx. 16, 19, 25, 31, 35, 41, 46, 50, 55, 96, 117 and 160 kDa. At the 48 h time point, all bands except for the 31 kDa band were observed. At the 96 h and 144 h time points, all bands except for the 50 kDa band were observed (Figure 3E–G). Overall, at least twelve xylan-degrading protein isoforms could be observed in these zymograms of approx. sizes 16, 19, 25, 31, 35, 41, 46, 50, 55, 96, 117 and 160 kDa at the 48, 96 and 144 h time points (Figure 3E–G), with a potential thirteenth band of approx. 65 kDa present on the β -D-xylosidase gel (Figure 3A,B). Furthermore, twelve bands were observed to have β -D-xylanase activity (Figure 3E–G), while four bands were observed to have β -D-xylosidase activity (Figure 3B).

E. maritima SFI-D6's xylan-degrading enzyme secretome profile when grown on WB during LSF is represented in Figure 3. In the zymogram testing for β -D-xylosidase activity, in the 48 h time point lanes, four active bands were visible at approx. 35, 46, 55 and 70 kDa when compared to the silver-stained gel (Figure 3C,D, lanes 1 and 2). In the lanes containing the protein samples from the 96 h and 144 h time points, these bands were also present, along with three other bands of approx. sizes 65, 160 and >250 kDa when compared to the silver-stained gel (Figure 3C,D, lanes 3–6). The bands of approx. 35, 46, 55, 65 and 70 kDa were the most concentrated in the 96 h time-point sample lanes, when compared to the 48 h and 144 h time-point lanes, while the activity bands of approx. 160 and >250 kDa were the most concentrated in the 144 h time-point lanes (Figure 3C,D, lanes 1–6). This zymogram, therefore, showed that during LSF on WB, this fungal isolate produced seven β -D-xylosidase activity bands. It either favoured the secretion of lower molecular weight β -D-xylosidases at the 48 h and 96 h time points and the production of larger β -D-xylosidase proteins at the 144 h time point, or it may instead be the case that multiple subunits of the same β -D-xylosidase complex are being visualised on the gel, as mentioned previously.

When testing for β -D-xylanase activity, ten activity bands at approx. 16, 19, 25, 31, 46, 55, 96, 117, 160 and >250 kDa were visible. All bands except for those of approx. sizes 19, 31, 46 and 55 kDa were visible in all lanes, and therefore were produced at all of the three time points analysed (Figure 3H, lanes 1–6). The 19, 31, 46 and 55 kDa bands were visible only in the 96 h and 144 h time-point lanes (Figure 3H, lanes 3–6). All bands visible in the gel increased in intensity over time, and therefore it was concluded that the concentration of the xylanolytic proteins being produced by the isolate increased over time.

Overall, it appeared that at least ten xylan-degrading proteins were secreted by *E. maritima* SFI-D6 at the 48 h, 96 h and 144 h time points. They were approx. 16, 19, 25, 31, 46, 55, 96, 117, 160 and >250 kDa in size (Figure 3H). There were three bands of approx. sizes 35, 65 and 70 kDa present on the β -D-xylosidase gel, which, if confirmed to be independent of those present on the β -D-xylanase gel, would bring the total of xylan-active protein bands to thirteen (Figure 3C,D). Overall, it was observed that ten bands had β -D-xylanase activity (Figure 3H), and seven bands had β -D-xylosidase activity (Figure 3C,D).

Both *E. maritima* isolates characterised in this study produced xylan-degrading proteins of approx. 16, 19, 25, 31, 35, 46, 55, 65, 96, 117 and 160 kDa (Figure 3). To date, studies with *Emericellopsis* sp. have focused on the production of novel antimicrobial and cytotoxic compounds [63–68].

Relatively little research has been carried out to describe the biomass-degrading activities of *Emericellopsis* sp. A previous study of the secretome of a marine *Emericellopsis* sp. TS11 showed xylanase-active bands of approx. 10 and 100 kDa via zymogram analysis when grown on wheat straw and corn stover [7], while other studies have determined that *Emericellopsis* sp. produce extracellular xylan- or biomass-degrading enzymes using media-based qualitative techniques and genomic and metabolomic techniques [20,49,69,70]. The novel marine strain *E. cladophorae* TS7 had its full genome sequenced, and this showed that it encoded genes for fourteen β -D-xylosidases from the GH43 family, two xylanases from the GH11 and four xylanases from the GH10 families [20], while the genome sequence

of *E. cladorporae* showed that some of the most abundant GH family-encoding genes were for β -D-xylosidases [71].

Overall, the strains of *E. maritima* produced at least twelve (SFI-F16) or ten (SFI-D6) xylan-degrading proteins each active against birchwood xylan or 4MUX (Figure 3). Similar numbers of xylanolytic enzyme isoforms were reportedly produced for *P. oxalicum* GZ-2 (14 isoforms), *T. emersonii* CBS814.70 (14 isoforms) and *Aspergillus fumigatus* SK1 (10 isoforms), respectively [72–74]. Other xylanolytic fungi have been shown to produce far fewer xylan-degrading isoforms using zymogram identification [75–81].

In order to effectively degrade the heteropolymeric D-xylan in nature, xylanases with similar but different substrate specificities are required [82,83]. Therefore, the *E. maritima* strains investigated in this study may be considered valuable sources of xylanolytic enzymes due to the amount of xylan-degrading isoforms produced over a wide size range. In particular, the number of β -D-xylosidases produced by *Emericellopsis* sp. was relatively large in comparison to other fungi [84], including all of the other isolates characterised in this paper.

P. chrysogenum SFI-D13's xylan-degrading secretome profile when grown on WB during LSF is represented in Figure 4A–C. When testing for β -D-xylosidase activity, one band of approx. 130 kDa was observed. It was clear that the concentration of this protein increased over time as the intensity of the band increased, with the most β -D-xylosidase being produced at the 144 h time point when compared to the silver-stained gel (Figure 4A,B). When testing for β -D-xylanase activity, four bands of approx. 35, 45, 60 and 64 kDa were observed. There was also a zone of clearance >70 kDa (Figure 4C, lanes 1–12). The 35 kDa band was present across all three time points, while the bands of size 45, 60 and 64 kDa were visible at the 96 h and 144 h time points only. The bands of size 45 and 60 kDa also showed a spread-out clearance zone, with the intensity of the clearance being largest at the 96 h time point (Figure 4C, lanes 9–12). This showed that the production of β -D-xylanase was most concentrated at the 96 h time point. Overall, five active xylanolytic enzymes appeared to be secreted by this isolate, with activity against xylan and 4MUX over the time points analysed, with β -D-xylanase being secreted the most at 96 h, and β -D-xylosidase at 144 h time point.

P. chrysogenum BBW2's xylan-degrading secretome profile when grown on WB during LSF is represented in Figure 4D–F. When testing for β -D-xylosidase activity, two bands of approx. 130 and ≥ 250 kDa were present when compared to the silver-stained gel (Figure 4D,E). When testing for β -D-xylanase activity, three bands of approx. sizes 35, 45 and 60 kDa were observed. There was also a zone of clearance visible >70 kDa. For this isolate, both the β -D-xylanase and β -D-xylosidase activities were the strongest at the 96 h and 144 h time points, with the least activity being observed at the 48 h time point (Figure 4D–F).

P. antarcticum SFI-F25's xylan-degrading enzyme secretome profile when grown on WB during LSF is represented in Figure 4G–I. When testing for β -D-xylosidase activity, a band of approx. 130 kDa was observed at the 144 h time point, when compared to the silver-stained gel (Figure 4G,H). This showed that this isolate favoured the secretion of β -D-xylosidase later at the 144 h time point during LSF on WB. When testing for β -D-xylanase, a band of approx. 45 kDa was observed. The band intensity appeared similar across all time points measured, indicating that the concentration of this enzyme secreted remained stable throughout the LSF. There was also a zone of clearance present >130 kDa, indicating β -D-xylanase activity in a protein of higher relative molecular size (Figure 4I).

In relation to β -D-xylosidase activity (Figure 4B,E,H), all three of the *Penicillium* isolates possessed an activity band at approx. 130 kDa when compared to their respective silver-stained gels. In addition to this, SFI-D13 produced a further β -D-xylosidase band ≥ 250 kDa. When comparing β -D-xylanase activity, all three isolates produced an activity band of approx. 45 kDa. In addition, *P. chrysogenum* SFI-D13 and BBW2 both produced activity bands at approx. 35 and 60 kDa, which were not produced by the *P. antarcticum* isolate. Only *P. chrysogenum* SFI-D13 produced an activity band at approx. 64 kDa.

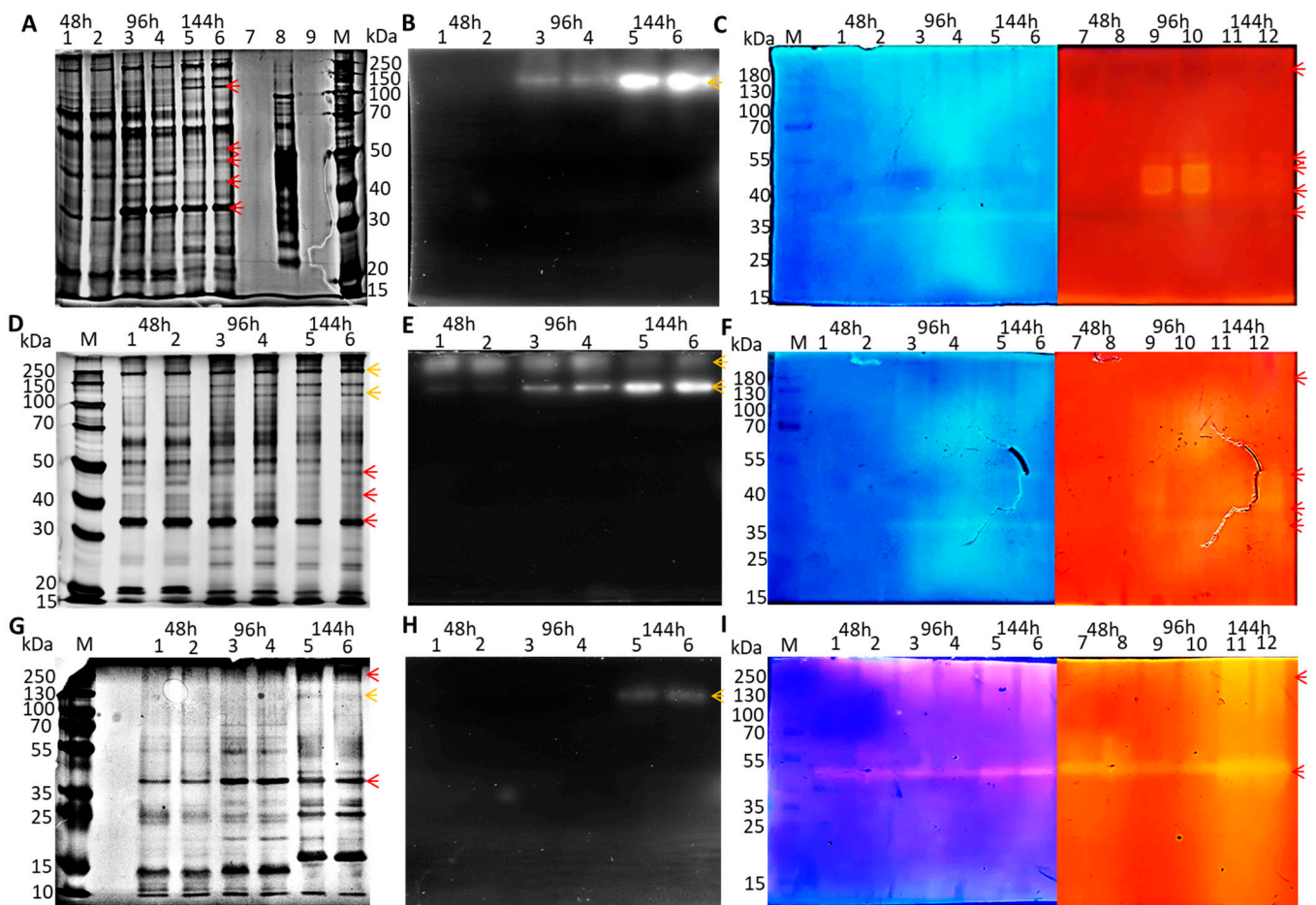


Figure 4. Xylanase secretome profiles of *P. chrysogenum* SFI-D13 (A–C), BBW2 (D–F) and *P. antarcticum* SFI-F25 (G–I) when grown on WB during LSF are presented in this figure. (A,D,G) are 10% ((A) and (D)) or 8% (G) silver-stained gels of the isolate secretomes at the sampled time points (1 and 2 = 48 h; 3 and 4 = 96 h; 5 and 6 = 144 h; 8 = control (only in (A))); M = molecular weight ladder), each with 10 µg of protein loaded/well; (B,E,H) are 10% ((B) and (E)) or 8% (G) zymograms incubated with the fluorescent 4MUX substrate and 40 µg of protein loaded per lane (1 and 2 = 48 h; 3 and 4 = 96 h; 5 and 6 = 144 h); (C,F,I) are 10% ((C) and (F)) or 8% (I) zymograms with in-gel xylan substrate (20 µg of protein loaded/well), before (right) and after (left) band enhancement with 1 M HCl (1 and 2/7 and 8 = 48 h; 3 and 4/ 9 and 10 = 96 h; 5 and 6/11 and 12 = 144 h). Yellow arrows signify β-D-xylosidase active bands. Red arrows signify β-D-xylanase active bands. Original images of the gels are available in Supplementary File S3.

P. chrysogenum has previously been reported to produce between one and three endo-β-D-xylanases when grown on inducing substrates, and up to three exo-β-D-xylosidases, similar to the three *Penicillium* isolates reported in this study [22,23,57,84–86]. Research published relating to *P. antarcticum*, however, has been limited [26,27]. To the best of the authors’ knowledge, the β-D-xylanase proteins from *P. antarcticum* have not been studied previously, so, therefore, an intra-isolate comparison for this isolate was not possible.

T. stollii SFI-F17’s xylan-degrading secretome profile when grown on WB during LSF is represented in Figure 5. When testing for β-D-xylosidase activity, three activity bands were present over the three time points when compared to the silver-stained gel, with the concentration of each band increasing from 48 h to 144 h. The bands were approx. 80, 130 and 250 kDa (Figure 5A,B). Notably, much less protein (10 µg/well) was required for band visibility on the β-D-xylosidase activity gel than was required for all of the other isolates studied in this paper, which supported the fact that the *T. stollii* isolate showed much

greater levels of β -D-xylosidase activity against the 4-NP- β -D-xylopyranoside substrate (see Section 3.2).

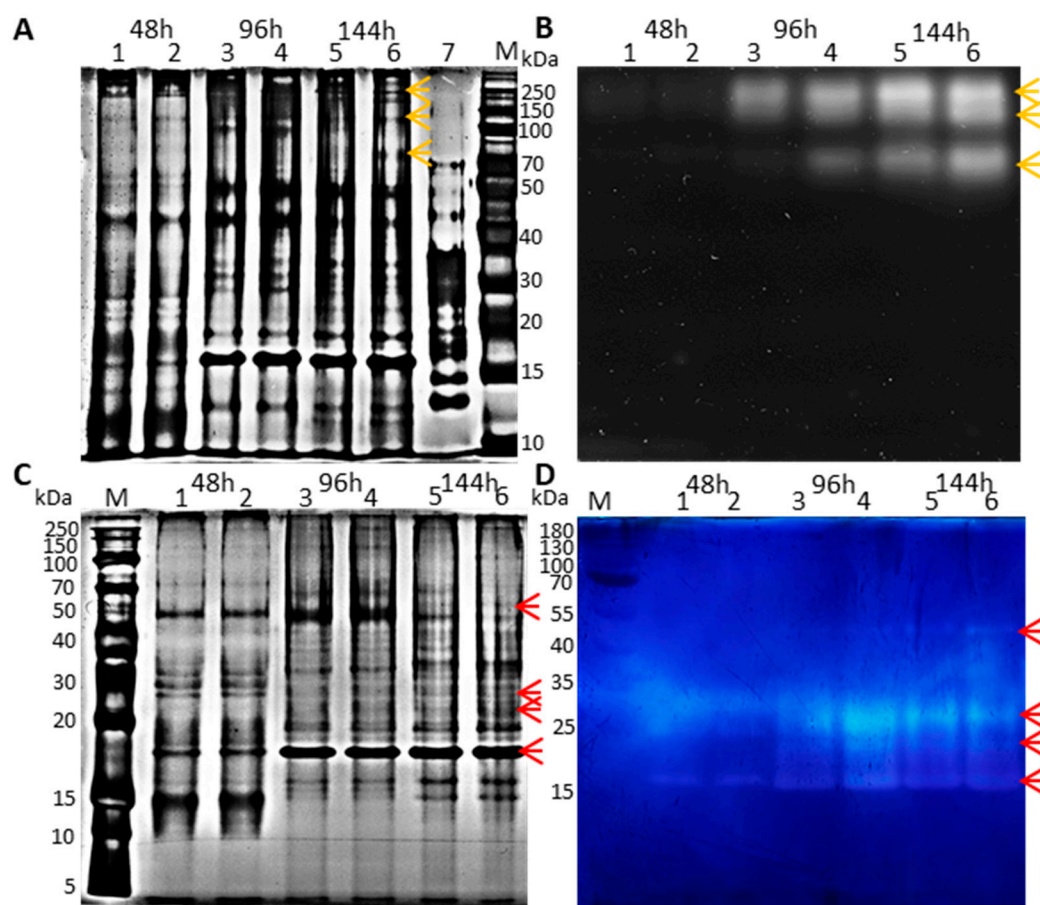


Figure 5. Xylanase secretome profile of *T. stollii* SFI-F17 when grown on WB during LSF is represented in this figure. (A) is an 8% silver stained gel of the isolate secretome at the sampled time points (1 and 2 = 48 h; 3 and 4 = 96 h; 5 and 6 = 144 h; 7 = control; M = molecular weight ladder); (B) is an 8% zymogram incubated with the fluorescent 4-MUX substrate and 10 μ g of protein loaded per lane (1 and 2 = 48 h; 3 and 4 = 96 h; 5 and 6 = 144 h); (C) is a 10% silver stained gel of the isolate secretome at the sampled time points (1 and 2 = 48 h; 3 and 4 = 96 h; 5 and 6 = 144 h; M = molecular weight ladder); and (D) is a 10% gel zymogram with in-gel xylan substrate (10 μ g of protein loaded/well) after band enhancement with 1 M HCl (1 and 2 = 48 h; 3 and 4 = 96 h; 5 and 6 = 144 h). Yellow arrows signify β -D-xylosidase active bands. Red arrows signify β -D-xylanase active bands. Original gel images are available in Supplementary File S3.

When testing for β -D-xylanase activity, four bands of approx. 17, 23, 29 and 50 kDa were observed across the three time points. All four bands were observed at the 96 h and 144 h time points, with the 96 h time point showing the most intensely active bands, suggesting the most active β -D-xylanase enzymes were produced at this time point. At the 48 h time point, the 17 and 29 kDa bands were observed, but not the 23 or 50 kDa bands. Overall, this isolate appeared to produce four β -D-xylanase bands and three β -D-xylosidase bands.

To date, few studies have described any enzymatic activities or specifically the production of cellulases and/or hemicellulases by *T. stollii*. *T. stollii* LV186 was isolated from corn stover treated with acid [48] and was shown to produce xylanase, β -D-xylosidase, β -D-glucosidase and glucanase activity. Studies of *T. emersonii* reported β -D xylanases of 17.5, 30.1, 35.7, 36.6, 45, 47.9, 48.6, 52.8, 54, 54.3, 58.5, 59 and 131 kDa and a β -D-xylosidase of 181 kDa [72,87]. *T. thermophilus* was reported to produce a β -D-xylanase of 25 kDa [48]

and a β -D-xylosidase of 97 kDa [88], while a β -D-xylosidase of 200 kDa and a β -D- of 19.8 kDa was reportedly produced by *T. amestolkiae* [25,88].

Further characterization of the xylanolytic enzymes produced by *T. stollii* SFI-F17 would be beneficial to more clearly define its xylanase secretion profile, such as, for example, by de novo sequencing of the isolate's secretome, or purification of specific enzymes using chromatographic methods like those reported in [72] and [55].

It is important to note that three of the limitations of these experiments were (a) the fact that a high concentration of protein was needed for the β -D-xylosidase activity zymogram and, therefore, it is possible that not all β -D-xylosidase-active proteins may have been detected if they were in low concentrations; (b) the fact that the sizes of the proteins are approximations, so the proteins may, in reality, be slightly different sizes than what was reported here; and (c) there may be more than one xylanolytic enzyme of the same size produced by the same isolate. These enzymes would not be separated using this gel format (2D-PAGE would be required) [89]. To know the exact sizes and specificities of xylanolytic enzymes produced by these two isolates, 2D-PAGE or de novo sequencing of their secretomes would be the next logical step [90,91].

4. Conclusions

In this study, five deep-sea fungi and one terrestrial fungus were analysed in detail for their lignocellulolytic capabilities. This study is the first to quantitatively characterise xylanase activities and exo-glycoside hydrolase activities secreted by *E. maritima*, *P. antarcticum* and a marine *T. stollii* strain. This study is also the first to quantitatively characterise xylanase activities by a marine strain of *P. chrysogenum* during LSF.

The secretomes of *E. maritima* SFI-F16 and SFI-D6, *P. chrysogenum* SFI-D13 and BBW2, *P. antarcticum* SFI-F25 and *T. stollii* SFI-F17 had xylanase volumetric activities of 49, 51, 152, 181, 20 and 13.2 IU·mL⁻¹. The xylanases functioned over a range of pH and temperatures, the most notable being those secreted by *E. maritima* SFI-F16 (alkalitolerant) and *T. stollii* SFI-F17 (acidophilic). The least versatile xylanase secretome in terms of temperature and pH was the terrestrial *P. chrysogenum* BBW2. Improved xylanase flexibility of *P. chrysogenum* was demonstrated in response to environmental stressors (pH and temperature variations) when produced by the marine strain compared to the terrestrial strain, making the xylanases produced by the marine strain more robust and potentially more suitable for biomass degradation purposes in industry. All isolates studied produced cold-active xylanases.

The isolates produced at least twelve, ten, five, five, three and seven bands exhibiting xylanase activity when zymogram analysis was carried out to test for exo- and endo-acting xylanase activities. The greatest number of xylanase active protein bands was produced by the *E. maritima* SFI-F16 and SFI-D6. Notably, strain SFI-D6 produced seven exo-acting β -D-xylosidase activity bands, far more than all of the other isolates in this study. The *E. maritima* strains produced a number of xylanase and β -xylosidase isomers comparable to those produced by *P. oxalicum* and *T. emersonii*, both of which are commercially used to produce lignocellulolytic enzyme cocktails.

The deep-sea *E. maritima* isolates produced a large number of xylanase and exo-glycoside hydrolase activities and produced more β -D-glucosidase, α -L-arabinofuranosidase and β -D-cellobiosidase activity than any other exo-activity.

The *P. chrysogenum* strains produced more β -D-glucosidase, β -D-galactosidase and β -D-xylosidase than any other exo-activity.

The *P. antarcticum* strain produced more β -D-xylosidase than any other exo-activity, with a relatively large β -D-mannosidase activity also being produced at 132 h.

T. stollii produced far higher combined levels of exo-acting glycoside hydrolase activities than all of the other isolates in this study, with a combined total of 8.02 IU·mL⁻¹ at the peak-production time point. *E. maritima* SFI-F16 and SFI-D6 produced combined totals of 3.58 IU·mL⁻¹ and 1.99 IU·mL⁻¹, while *P. chrysogenum* SFI-D13 and BBW2 produced combined totals of 3.07 IU·mL⁻¹ and 3.38 IU·mL⁻¹.

Exo-glycoside hydrolase levels produced by natural strains of filamentous fungi under unoptimised conditions are typically low, and in many cases lower than levels produced by *T. stollii* and reported in this study. Although the levels of these activities may seem to be low, their combined effect in synergistic interaction could greatly enhance lignocellulose bioconversion. *T. stollii* SFI-F17 may therefore be an excellent candidate for industrial uses, such as lignocellulose waste hydrolysis prior to biofuel production.

Supplementary Materials: The following supporting information can be downloaded at: <https://www.mdpi.com/article/10.3390/fermentation9090780/s1>. Supplementary File S1: file with statistical calculations. Supplementary File S2: Supplementary Figures S1 and S2. Supplementary File S3: file with original gel images for Figures S3–S5.

Author Contributions: Conceptualization, B.D. and M.G.T.; methodology, B.D. and M.G.T.; validation, B.D. and M.G.T.; formal analysis, B.D.; investigation, B.D.; resources, M.G.T.; data curation, B.D.; writing—original draft preparation, B.D.; writing—review and editing, B.D. and M.G.T.; visualization, B.D.; supervision, M.G.T.; project administration, M.G.T.; funding acquisition, M.G.T. All authors have read and agreed to the published version of the manuscript.

Funding: This research was funded by Science Foundation Ireland (SFI) through MaREI, the SFI Research Centre for Energy, Climate, and Marine (Grant No: 12/RC/2302_16/SP/3829), with supporting funding obtained from the ABP Food Group.

Institutional Review Board Statement: Not applicable.

Informed Consent Statement: Not applicable.

Data Availability Statement: Data is available upon request from the authors.

Acknowledgments: The authors are thankful to the funders of this project, the Science Foundation of Ireland and ABP Food Group, and to colleagues in the Sustainable Energy and Fuel Efficiency (SEFE) Spoke, MaREI and Energy research clusters in the Ryan Institute, University of Galway. The authors wish to acknowledge the contribution of Louise Allcock, Ryan Young and Pietro Marchese in deep-sea sample collection, fungal isolate purification and identification.

Conflicts of Interest: The authors declare no conflict of interest.

References

1. Birolli, W.G.; Lima, R.N.; Porto, A.L.M. Applications of Marine-Derived Microorganisms and Their Enzymes in Biocatalysis and Biotransformation, the Underexplored Potentials. *Front. Microbiol.* **2019**, *10*, 1453. [[CrossRef](#)] [[PubMed](#)]
2. Chávez, R.; Fierro, F.; García-Rico, R.O.; Vaca, I. Filamentous Fungi from Extreme Environments as a Promising Source of Novel Bioactive Secondary Metabolites. *Front. Microbiol.* **2015**, *6*, 903. [[CrossRef](#)]
3. Marchese, P.; Garzoli, L.; Young, R.; Allcock, L.; Barry, F.; Tuohy, M.; Murphy, M. Fungi Populate Deep-Sea Coral Gardens as Well as Marine Sediments in the Irish Atlantic Ocean. *Environ. Microbiol.* **2021**, *23*, 4168–4184. [[CrossRef](#)] [[PubMed](#)]
4. Coleine, C.; Stajich, J.E.; Selbmann, L. Fungi Are Key Players in Extreme Ecosystems. *Trends Ecol. Evol.* **2022**, *37*, 517–528. [[CrossRef](#)] [[PubMed](#)]
5. Nagano, Y.; Nagahama, T. Fungal Diversity in Deep-Sea Extreme Environments. *Fungal Ecol.* **2012**, *5*, 463–471. [[CrossRef](#)]
6. Rédou, V.; Navarri, M.; Meslet-Cladière, L.; Barbier, G.; Burgaud, G. Species Richness and Adaptation of Marine Fungi from Deep-Subseafloor Sediments. *Appl. Environ. Microbiol.* **2015**, *81*, 3571–3583. [[CrossRef](#)]
7. Batista-García, R.A.; Sutton, T.; Jackson, S.A.; Tovar-Herrera, O.E.; Balcázar-López, E.; del Rayo Sánchez-Carbente, M.; Sánchez-Reyes, A.; Dobson, A.D.W.; Folch-Mallol, J.L. Characterization of Lignocellulolytic Activities from Fungi Isolated from the Deep-Sea Sponge *Stelletta normani*. *PLoS ONE* **2017**, *12*, e0173750. [[CrossRef](#)]
8. Hu, X.Y.; Li, X.M.; Wang, B.G.; Meng, L.H. Tazawaic Acid Derivatives: Fungal Polyketides from the Deep-Sea Coral-Derived Endozoic *Penicillium steckii* AS-324. *J. Nat. Prod.* **2022**, *85*, 1398–1406. [[CrossRef](#)]
9. Cheng, Z.; Liu, W.; Fan, R.; Han, S.; Li, Y.; Cui, X.; Zhang, J.; Wu, Y.; Lv, X.; Zhang, Y.; et al. Terpenoids from the Deep-Sea-Derived Fungus *Penicillium thomii* YPGA3 and Their Bioactivities. *Mar. Drugs* **2020**, *18*, 164. [[CrossRef](#)]
10. Limbadri, S.; Luo, X.; Lin, X.; Liao, S.; Wang, J.; Zhou, X.; Yang, B.; Liu, Y. Bioactive Novel Indole Alkaloids and Steroids from Deep Sea-Derived Fungus *Aspergillus fumigatus* SCSIO 41012. *Molecules* **2018**, *23*, 2379. [[CrossRef](#)]
11. Andlar, M.; Rezić, T.; Marđetko, N.; Kracher, D.; Ludwig, R.; Šantek, B. Lignocellulose Degradation: An Overview of Fungi and Fungal Enzymes Involved in Lignocellulose Degradation. *Eng. Life Sci.* **2018**, *18*, 768–778. [[CrossRef](#)] [[PubMed](#)]

12. Abdeshahian, P.; Kadier, A.; Rai, P.K.; Silva, S.S. Lignocellulose as a Renewable Carbon Source for Microbial Synthesis of Different Enzymes. In *Lignocellulosic Biorefining Technologies*; Ingle, A.P., Chandel, A.K., da Silva, S.S., Eds.; John Wiley & Sons Ltd.: Hoboken, NJ, USA, 2020; pp. 185–202.
13. Howard, R.L.; Abotsi, E.; Van Rensburg, E.L.J.; Howard, S. Lignocellulose Biotechnology: Issues of Bioconversion and Enzyme Production. *Afr. J. Biotechnol.* **2003**, *2*, 702–733. [[CrossRef](#)]
14. Smith, M.D. An Abbreviated Historical and Structural Introduction to Lignocellulose. In *Understanding Lignocellulose: Synergistic Computational and Analytic Methods*; American Chemical Society: Washington, DC, USA, 2019; Volume 1338, pp. 1–15. [[CrossRef](#)]
15. Dowd, B.; McDonnell, D.; Tuohy, M.G. Current Progress in Optimising Sustainable Energy Recovery From Cattle Paunch Contents, a Slaughterhouse Waste Product. *Front. Sustain. Food Syst.* **2022**, *6*, 722424. [[CrossRef](#)]
16. Saini, J.K.; Saini, R.; Tewari, L. Lignocellulosic Agriculture Wastes as Biomass Feedstocks for Second-Generation Bioethanol Production: Concepts and Recent Developments. *3 Biotech* **2015**, *5*, 337–353. [[CrossRef](#)] [[PubMed](#)]
17. Raghukumar, C.; Muraleedharan, U.; Gaud, V.R.; Mishra, R. Xylanases of Marine Fungi of Potential Use for Biobleaching of Paper Pulp. *J. Ind. Microbiol. Biotechnol.* **2004**, *31*, 433–441. [[CrossRef](#)] [[PubMed](#)]
18. Damare, S.; Raghukumar, C.; Muraleedharan, U.D.; Raghukumar, S. Deep-Sea Fungi as a Source of Alkaline and Cold-Tolerant Proteases. *Enzyme Microb. Technol.* **2006**, *39*, 172–181. [[CrossRef](#)]
19. National Oceanic and Atmospheric Administration-Ocean Acidification. Available online: <https://www.noaa.gov/education/resource-collections/ocean-coasts/ocean-acidification> (accessed on 15 June 2023).
20. Hagestad, O.C.; Hou, L.; Andersen, J.H.; Hansen, E.H.; Altermark, B.; Li, C.; Kuhnert, E.; Cox, R.J.; Crous, P.W.; Spatafora, J.W.; et al. Genomic Characterization of Three Marine Fungi, Including *Emericellopsis atlantica* Sp. Nov. with Signatures of a Generalist Lifestyle and Marine Biomass Degradation. *IMA Fungus* **2021**, *12*, 21. [[CrossRef](#)]
21. Ruginescu, R.; Enache, M.; Popescu, O.; Gomoiu, I.; Cojoc, R.; Batrinescu-Moteau, C.; Maria, G.; Dumbravician, M.; Neagu, S. Characterization of Some Salt-Tolerant Bacterial Hydrolases with Potential Utility in Cultural Heritage Bio-Cleaning. *Microorganisms* **2022**, *10*, 644. [[CrossRef](#)]
22. Terrone, C.C.; de Freitas, C.; Terrasan, C.R.F.; de Almeida, A.F.; Carmona, E.C. Agroindustrial Biomass for Xylanase Production by *Penicillium chrysogenum*: Purification, Biochemical Properties and Hydrolysis of Hemicelluloses. *Electron. J. Biotechnol.* **2018**, *33*, 39–45. [[CrossRef](#)]
23. Yang, Y.; Yang, J.; Wang, R.; Liu, J.; Zhang, Y.; Liu, L.; Wang, F.; Yuan, H. Cooperation of Hydrolysis Modes among Xylanases Reveals the Mechanism of Hemicellulose Hydrolysis by *Penicillium chrysogenum* P33. *Microb. Cell Fact.* **2019**, *18*, 159. [[CrossRef](#)]
24. Haas, H.; Herfurth, E.; Stöffler, G.; Redl, B. Purification, Characterization and Partial Amino Acid Sequences of a Xylanase Produced by *Penicillium chrysogenum*. *Biochim. Biophys. Acta Gen. Subj.* **1992**, *1117*, 279–286. [[CrossRef](#)]
25. Ullah, S.F.; Souza, A.A.; Hamann, P.R.V.; Ticona, A.R.P.; Oliveira, G.M.; Barbosa, J.A.R.G.; Freitas, S.M.; Noronha, E.F. Structural and Functional Characterisation of Xylanase Purified from *Penicillium chrysogenum* Produced in Response to Raw Agricultural Waste. *Int. J. Biol. Macromol.* **2019**, *127*, 385–395. [[CrossRef](#)]
26. Leshchenko, E.V.; Antonov, A.S.; Borkunov, G.V.; Hauschild, J.; Zhuravleva, O.I.; Khudyakova, Y.V.; Menshov, A.S.; Popov, R.S.; Kim, N.Y.; Graefen, M.; et al. New Bioactive β -Resorcylic Acid Derivatives from the Alga-Derived Fungus *Penicillium antarcticum* KMM 4685. *Mar. Drugs* **2023**, *21*, 178. [[CrossRef](#)] [[PubMed](#)]
27. Leshchenko, E.V.; Antonov, A.S.; Dyshlovoy, S.A.; Berdyshev, D.V.; Hauschild, J.; Zhuravleva, O.I.; Borkunov, G.V.; Menshov, A.S.; Kirichuk, N.N.; Popov, R.S.; et al. Meroantarctines A-C, Meroterpenoids with Rearranged Skeletons from the Alga-Derived Fungus *Penicillium antarcticum* KMM 4685 with Potent p-Glycoprotein Inhibitory Activity. *J. Nat. Prod.* **2022**, *85*, 2746–2752. [[CrossRef](#)] [[PubMed](#)]
28. Cheng, L.; Zhang, H.; Cui, H.; Davari, M.D.; Wei, B.; Wang, W.; Yuan, Q. Efficient Enzyme-Catalyzed Production of Diosgenin: Inspired by the Biotransformation Mechanisms of Steroid Saponins in: *Talaromyces stollii* CLY-6. *Green Chem.* **2021**, *23*, 5896–5910. [[CrossRef](#)]
29. Waters, D.M.; Murray, P.G.; Ryan, L.A.; Arendt, E.K.; Tuohy, M.G. *Talaromyces Emersonii* Thermostable Enzyme Systems and Their Applications in Wheat Baking Systems. *J. Agric. Food Chem.* **2010**, *58*, 7415–7422. [[CrossRef](#)]
30. Miller, G.L. Use of Dinitrosalicylic Acid Reagent for Determination of Reducing Sugar. *Anal. Chem.* **1959**, *31*, 426–428. [[CrossRef](#)]
31. Pointing, S.B. Qualitative Methods for the Determination of Lignocellulolytic Enzyme Production by Tropical Fungi. *Fungal Divers.* **1999**, *2*, 17–33.
32. Pan, D.; Wilson, K.A.; Tan-Wilson, A. Transfer Zymography. *Methods Mol. Biol.* **2017**, *1626*, 253–269. [[CrossRef](#)]
33. McCarthy, T.; Tuohy, M.G. A Multi-Step Chromatographic Strategy to Purify Three Fungal Endo- β -Glucanases. *Methods Mol. Biol.* **2011**, *681*, 497–524. [[CrossRef](#)]
34. Grudkowska, M.; Lisik, P.; Rybka, K. Two-dimensional zymography in detection of proteolytic enzymes in wheat leaves. *Acta Physiol. Plant.* **2013**, *35*, 3477–3482. [[CrossRef](#)]
35. Minic, Z.; Jouanin, L. Plant Glycoside Hydrolases Involved in Cell Wall Polysaccharide Degradation. *Plant Physiol. Biochem.* **2006**, *44*, 435–449. [[CrossRef](#)]
36. Olfa, E.; Mondher, M.; Issam, S.; Ferid, L.; Nejib, M.M. Induction, Properties and Application of Xylanase Activity from *Sclerotinia sclerotiorum* S2 Fungus. *J. Food Biochem.* **2007**, *31*, 96–107. [[CrossRef](#)]
37. Gaffney, M.; Doyle, S.; Murphy, R. Optimization of Xylanase Production by *Thermomyces lanuginosus* in Solid State Fermentation. *Biosci. Biotechnol. Biochem.* **2009**, *73*, 2640–2644. [[CrossRef](#)]

38. Kumar, B.A.; Amit, K.; Alok, K.; Dharm, D. Wheat Bran Fermentation for the Production of Cellulase and Xylanase by *Aspergillus niger* NFCCI 4113. *Res. J. Biotechnol.* **2018**, *13*, 11–18.
39. Barbieri, G.S.; Bento, H.B.S.; de Oliveira, F.; Picheli, F.P.; Dias, L.M.; Masarin, F.; Santos-Ebinuma, V.C. Xylanase Production by *Talaromyces amestolkiae* Valuing Agroindustrial Byproducts. *BioTech* **2022**, *11*, 15. [[CrossRef](#)]
40. Shuster, L. Repression and De-Repression of Enzyme Synthesis as a Possible Explanation of some Aspects of Drug Action. *Nature* **1961**, *189*, 314–315. [[CrossRef](#)]
41. Purkarthofer, H.; Sinner, M.; Steiner, W. Cellulase-free xylanase from Optimization of production in *Thermomyces lanuginosus*: Submerged and solid-state culture. *Enzyme Microb. Technol.* **1993**, *15*, 677–682. [[CrossRef](#)]
42. Mach-Aigner, A.R.; Pucher, M.E.; Mach, R.L. D-Xylose as a Repressor or Inducer of Xylanase Expression in *Hypocrea jecorina* (*Trichoderma reesei*). *Appl. Environ. Microbiol.* **2010**, *76*, 1770–1776. [[CrossRef](#)]
43. Daly, P.; Peng, M.; Di Falco, M.; Lipzen, A.; Wang, M.; Ng, V.; Grigoriev, I.V.; Tsang, A.; Mäkelä, M.R.; de Vries, R.P. Glucose-Mediated Repression of Plant Biomass Utilization in the White-Rot Fungus *Dichomitus squalens*. *Appl. Environ. Microbiol.* **2019**, *85*, e01828-19. [[CrossRef](#)] [[PubMed](#)]
44. Khanahmadi, M.; Arezi, I.; Amiri, M.S.; Miranzadeh, M. Bioprocessing of agro-industrial residues for optimization of xylanase production by solid- state fermentation in flask and tray bioreactor. *Biocatal. Agric. Biotechnol.* **2018**, *13*, 272–282. [[CrossRef](#)]
45. Okafor, U.A.; Emezue, T.N.; Okochi, V.I.; Onyegeme-Okerenta, B.M.; Nwodo-Chinedu, S. Xylanase Production by *Penicillium chrysogenum* (PCL501) Fermented on Cellulosic Wastes. *Afr. J. Biochem. Res.* **2007**, *1*, 48–053.
46. Bajaj, B.K.; Sharma, M.; Sharma, S. Alkalistable Endo- β -1,4-Xylanase Production from a Newly Isolated Alkalitolerant *Penicillium* Sp. SS1 Using Agro-Residues. *3 Biotech* **2011**, *1*, 83–90. [[CrossRef](#)]
47. Hou, Y.-H.; Wang, T.-H.; Long, H.; Zhu, H.-Y. Novel Cold-adaptive *Penicillium* Strain FS010 Secreting Thermo-labile Xylanase Isolated from Yellow Sea. *Acta Biochim. Biophys. Sin.* **2006**, *38*, 142–149. [[CrossRef](#)]
48. Orenco-Trejo, M.; Torres-Granados, J.; Rangel-Lara, A.; Beltrán-Guerrero, E.; García-Aguilar, S.; Moss-Acosta, C.; Valenzuela-Soto, H.; De la Torre-Zavala, S.; Gastelum-Arellanez, A.; Martinez, A.; et al. Cellulase and Xylanase Production by the Mexican Strain *Talaromyces stollii* LV186 and Its Application in the Saccharification of Pretreated Corn and Sorghum Stover. *Bioenergy Res.* **2016**, *9*, 1034–1045. [[CrossRef](#)]
49. Zuccaro, A.; Summerbell, R.C.; Gams, W.; Schroers, H.J.; Mitchell, J.I. A New *Acremonium* Species Associated with *Fucus* Spp., and Its Affinity with a Phylogenetically Distinct Marine *Emericellopsis* Clade. *Stud. Mycol.* **2004**, *50*, 283–297.
50. Petruccioli, M.; Fenice, M.; Piccioni, P. Distribution and Typology of Glucose Oxidase Activity in the Genus *Penicillium*. *Lett. Appl. Microbiol.* **1993**, *17*, 285–288. [[CrossRef](#)]
51. Hao, D.C.; Song, S.M.; Cheng, Y.; Qin, Z.Q.; Ge, G.B.; An, B.L.; Xiao, P.G. Functional and Transcriptomic Characterization of a Dye-Decolorizing Fungus from *Taxus* Rhizosphere. *Pol. J. Microbiol.* **2018**, *67*, 417–429. [[CrossRef](#)] [[PubMed](#)]
52. Bar-On, Y.M.; Phillips, R.; Milo, R. The biomass distribution on Earth. *Proc. Natl. Acad. Sci. USA* **2018**, *115*, 6506–6511. [[CrossRef](#)] [[PubMed](#)]
53. Cheng, L.; Zhang, H.; Cui, H.; Cheng, J.; Wang, W.; Wei, B.; Liu, F.; Liang, H.; Shen, X.; Yuan, Q. A Novel α -L-Rhamnosidase Renders Efficient and Clean Production of Icaritin. *J. Clean. Prod.* **2022**, *341*, 130903. [[CrossRef](#)]
54. Gil, J. Estudio de Las β -Glucosidasas Del Complejo Celulítico de *Talaromyces amestolkiae*: Caracterización y Aplicaciones Biotecnológicas. Ph.D. Thesis, Universidad Complutense, Madrid, Spain, 2015.
55. Nieto-Domínguez, M.; de Eugenio, L.I.; Barriuso, J.; Prieto, A.; Fernández de Toro, B.; Canales-Mayordomo, Á.; Martínez, M.J. Novel PH-Stable Glycoside Hydrolase Family 3 β -Xylosidase from *Talaromyces amestolkiae*: An Enzyme Displaying Regioselective Transxylosylation. *Appl. Environ. Microbiol.* **2015**, *81*, 6380–6392. [[CrossRef](#)]
56. Subramanian, S.; Prema, P. Biotechnology of Microbial Xylanases: Enzymology, Molecular Biology, and Application. *Crit. Rev. Biotechnol.* **2002**, *22*, 33–64. [[CrossRef](#)] [[PubMed](#)]
57. dos Reis, L.; Schneider, W.D.H.; Fontana, R.C.; Camassola, M.; Dillon, A.J.P. Cellulase and Xylanase Expression in Response to Different pH Levels of *Penicillium echinulatum* S1M29 Medium. *Bioenergy Res.* **2014**, *7*, 60–67. [[CrossRef](#)]
58. Sunkar, B.; Kannoju, B.; Bhukya, B. Optimized Production of Xylanase by *Penicillium purpurogenum* and Ultrasound Impact on Enzyme Kinetics for the Production of Monomeric Sugars From Pretreated Corn Cobs. *Front. Microbiol.* **2020**, *11*, 772. [[CrossRef](#)] [[PubMed](#)]
59. Kulkarni, N.; Shendye, A.; Rao, M. Molecular and Biotechnological Aspects of Xylanases. *FEMS Microbiol. Rev.* **1999**, *23*, 411–456. [[CrossRef](#)]
60. Bates, N.R.; Best, M.H.P.; Neely, K.; Garley, R.; Dickson, A.G.; Johnson, R.J. Detecting Anthropogenic Carbon Dioxide Uptake and Ocean Acidification in the North Atlantic Ocean. *Biogeosciences* **2012**, *9*, 2509–2522. [[CrossRef](#)]
61. Arif, A.R.; Natsir, H.; Rohani, H.; Karim, A. Effect of pH fermentation on production bioethanol from jackfruit seeds (*Artocarpus heterophyllus*) through separate fermentation hydrolysis method. *J. Phys. Conf. Ser.* **2018**, *979*, 012015. [[CrossRef](#)]
62. Corradini, F.A.S.; Milessi, T.S.; Gonçalves, V.M.; Ruller, R.; Sargo, C.R.; Lopes, L.A.; Zangirolami, T.C.; Tardioli, P.W.; Giordano, R.C.; Giordano, R.L.C. High stabilization and hyperactivation of a Recombinant β -Xylosidase through Immobilization Strategies. *Enzyme Microb. Technol.* **2021**, *145*, 109725. [[CrossRef](#)] [[PubMed](#)]
63. Kuvarina, A.E.; Gavryushina, I.A.; Kulko, A.B.; Ivanov, I.A.; Rogozhin, E.A.; Georgieva, M.L.; Sadykova, V.S. The Emericellipsins a-e from an Alkalophilic Fungus *Emericellopsis alkalina* Show Potent Activity against Multidrug-Resistant Pathogenic Fungi. *J. Fungi* **2021**, *7*, 153. [[CrossRef](#)]

64. Kuvarina, A.E.; Sukonnikov, M.A.; Rogozhin, E.A.; Serebryakova, M.V.; Timofeeva, A.V.; Georgieva, M.L.; Sadykova, V.S. Formation of Various Antimicrobial Peptide Emericellipsin Isoforms in *Emericellopsos alkalina* under Different Cultivation Conditions. *Appl. Biochem. Microbiol.* **2023**, *59*, 160–167. [[CrossRef](#)]
65. Kuvarina, A.E.; Gavryushina, I.A.; Sykonnikov, M.A.; Efimenko, T.A.; Markelova, N.N.; Bilanenko, E.N.; Bondarenko, S.A.; Kokaeva, L.Y.; Timofeeva, A.V.; Serebryakova, M.V.; et al. Exploring Peptaibol's Profile, Antifungal, and Antitumor Activity of Emericellipsin A of *Emericellopsis* Species from Soda and Saline Soils. *Molecules* **2022**, *27*, 1736. [[CrossRef](#)]
66. Rogozhin, E.A.; Sadykova, V.S.; Baranova, A.A.; Vasilchenko, A.S.; Lushpa, V.A.; Mineev, K.S.; Georgieva, M.L.; Kul'ko, A.B.; Krashennikov, M.E.; Lyundup, A.V.; et al. A Novel Lipopeptaibol Emericellipsin a with Antimicrobial and Antitumor Activity Produced by the Extremophilic Fungus *Emericellopsis alkalina*. *Molecules* **2018**, *23*, 2785. [[CrossRef](#)] [[PubMed](#)]
67. Abraúl, M.; Alves, A.; Hilário, S.; Melo, T.; Conde, T.; Domingues, M.R.; Rey, F. Evaluation of Lipid Extracts from the Marine Fungi *Emericellopsis cladophorae* and *Zalerion maritima* as a Source of Anti-Inflammatory, Antioxidant and Antibacterial Compounds. *Mar. Drugs* **2023**, *21*, 199. [[CrossRef](#)] [[PubMed](#)]
68. Agrawal, S.; Dufossé, L.; Deshmukh, S.K. Antibacterial Metabolites from an Unexplored Strain of Marine Fungi *Emericellopsis minima* and Determination of the Probable Mode of Action against *Staphylococcus aureus* and Methicillin-Resistant *S. aureus*. *Biotechnol. Appl. Biochem.* **2023**, *70*, 120–129. [[CrossRef](#)]
69. Gonçalves, M.F.M.; Paço, A.; Escada, L.F.; Albuquerque, M.S.F.; Pinto, C.A.; Saraiva, J.; Duarte, A.S.; Rocha-Santos, T.A.P.; Esteves, A.C.; Alves, A. Unveiling Biological Activities of Marine Fungi: The Effect of Sea Salt. *Appl. Sci.* **2021**, *11*, 6008. [[CrossRef](#)]
70. Gomoiu, I.; Cojoc, R.; Ruginescu, R.; Neagu, S.; Enache, M.; Maria, G.; Dumbrăvician, M.; Olteanu, I.; Rădvan, R.; Ratoiu, L.C.; et al. Brackish and Hypersaline Lakes as Potential Reservoir for Enzymes Involved in Decomposition of Organic Materials on Frescoes. *Fermentation* **2022**, *8*, 462. [[CrossRef](#)]
71. Gonçalves, M.F.M.; Hilário, S.; Van de Peer, Y.; Esteves, A.C.; Alves, A. Genomic and Metabolomic Analyses of the Marine Fungus *Emericellopsis cladophorae*: Insights into Saltwater Adaptability Mechanisms and Its Biosynthetic Potential. *J. Fungi* **2022**, *8*, 31. [[CrossRef](#)]
72. Tuohy, M.G.; Laffey, C.D.; Coughlan, M.P. Characterization of the Individual Components of the Xylanolytic Enzyme System of *Talaromyces emersonii*. *Bioresour. Technol.* **1994**, *50*, 37–42. [[CrossRef](#)]
73. Liao, H.; Xu, C.; Tan, S.; Wei, Z.; Ling, N.; Yu, G.; Raza, W.; Zhang, R.; Shen, Q.; Xu, Y. Production and Characterization of Acidophilic Xylanolytic Enzymes from *Penicillium oxalicum* GZ-2. *Bioresour. Technol.* **2012**, *123*, 117–124. [[CrossRef](#)]
74. Ang, S.K.; Shaza, E.M.; Adibah, Y.A.; Suraini, A.A.; Madihah, M.S. Production of Cellulases and Xylanase by *Aspergillus fumigatus* SK1 Using Untreated Oil Palm Trunk through Solid State Fermentation. *Process Biochem.* **2013**, *48*, 1293–1302. [[CrossRef](#)]
75. Miao, Y.; Li, J.; Xiao, Z.; Shen, Q.; Zhang, R. Characterization and Identification of the Xylanolytic Enzymes from *Aspergillus fumigatus* Z5. *BMC Microbiol.* **2015**, *15*, 126. [[CrossRef](#)] [[PubMed](#)]
76. Chipeta, Z.A.; du Preez, J.C.; Szakacs, J.; Christopher, L. Xylanase Production by Fungal Strains on Spent Sulphite Liquor. *Appl. Microbiol. Biotechnol.* **2005**, *69*, 71–78. [[CrossRef](#)] [[PubMed](#)]
77. Joshi, C.; Khare, S.K. Induction of Xylanase in Thermophilic Fungi *Scytalidium thermophilum* and *Sporotrichum Thermophile*. *Braz. Arch. Biol. Technol.* **2012**, *55*, 21–27. [[CrossRef](#)]
78. Lin, C.; Shen, Z.; Zhu, T.; Qin, W. Newly Isolated *Penicillium ramulosum* N1 Is Excellent for Producing Protease-Resistant Acidophilic Xylanase. *J. Mol. Microbiol. Biotechnol.* **2015**, *25*, 320–326. [[CrossRef](#)] [[PubMed](#)]
79. Badhan, A.K.; Chadha, B.S.; Sonia, K.G.; Saini, H.S.; Bhat, M.K. Functionally Diverse Multiple Xylanases of Thermophilic Fungus *Myceliophthora* Sp. IMI 387099. *Enzyme Microb Technol.* **2004**, *35*, 460–466. [[CrossRef](#)]
80. Sachslehner, A.; Nidetzky, B.; Kulbe, K.D.; Haltrich, D. Induction of Mannanase, Xylanase, and Endoglucanase Activities in *Sclerotium rolfsii*. *Appl. Environ. Microbiol.* **1998**, *64*, 594–600. [[CrossRef](#)]
81. Bachmann, S.L.; McCarthy, A.J. Purification and Cooperative Activity of Enzymes Constituting the Xylan-Degrading System of *Thermomonospora fusca*. *Appl. Environ. Microbiol.* **1991**, *57*, 2121–2130. [[CrossRef](#)]
82. Álvarez-Cervantes, J.; Domínguez-Hernández, E.M.; Mercado-Flores, Y.; O'Donovan, A.; Díaz-Godínez, G. Mycosphere Essay 10: Properties and Characteristics of Microbial Xylanases. *Mycosphere* **2016**, *7*, 1600–1619. [[CrossRef](#)]
83. Hong, P.Y.; Iakiviak, M.; Dodd, D.; Zhang, M.; Mackie, R.I.; Cann, I. Two New Xylanases with Different Substrate Specificities from the Human Gut Bacterium *Bacteroides intestinalis* DSM 17393. *Appl. Environ. Microbiol.* **2014**, *80*, 2084–2093. [[CrossRef](#)]
84. Knob, A.; Terrasan, C.R.F.; Carmona, E.C. β -Xylosidases from Filamentous Fungi: An Overview. *World J. Microbiol. Biotechnol.* **2010**, *26*, 389–407. [[CrossRef](#)]
85. Mamo, G.; Thunnissen, M.; Hatti-Kaul, R.; Mattiasson, B. An Alkaline Active Xylanase: Insights into Mechanisms of High pH Catalytic Adaptation. *Biochimie* **2009**, *91*, 1187–1196. [[CrossRef](#)]
86. Yang, Y.; Yang, J.; Liu, J.; Wang, R.; Liu, L.; Wang, F.; Yuan, H. The Composition of Accessory Enzymes of *Penicillium chrysogenum* P33 Revealed by Secretome and Synergistic Effects with Commercial Cellulase on Lignocellulose Hydrolysis. *Bioresour. Technol.* **2018**, *257*, 54–61. [[CrossRef](#)] [[PubMed](#)]
87. Tuohy, M.G.; Murray, G.P.; Gilleran, C.T.; Collins, C.T.; Reen, F.J.; McLoughlin, L.P.; Lydon, A.G.S.; Maloney, A.P.; Heneghan, M.N.; O'Donoghue, A.G.; et al. *Talaromyces emersonii* Xylanase. European Patent No. 11157751.6, 7 September 2011.
88. Guerfali, M.; Gargouri, A.; Belghith, H. *Talaromyces thermophilus* β -d-Xylosidase: Purification, Characterization and Xylobiose Synthesis. *Appl. Biochem. Biotechnol.* **2008**, *150*, 267–279. [[CrossRef](#)] [[PubMed](#)]

89. Roy, S.; Dutta, T.; Sarkar, T.S.; Ghosh, S. Novel Xylanases from *Simplicillium obclavatum* MTCC 9604: Comparative Analysis of Production, Purification and Characterization of Enzyme from Submerged and Solid State Fermentation. *SpringerPlus* **2013**, *2*, 382. [[CrossRef](#)] [[PubMed](#)]
90. Peterson, R.; Grinyer, J.; Nevalainen, H. Secretome of the Coprophilous Fungus *Doratomyces stemonitis* C8, Isolated from Koala Feces. *Appl. Environ. Microbiol.* **2011**, *77*, 3793–3801. [[CrossRef](#)]
91. Sethupathy, S.; Morales, G.M.; Li, Y.; Wang, Y.; Jiang, J.; Sun, J.; Zhu, D. Harnessing Microbial Wealth for Lignocellulose Biomass Valorization through Secretomics: A Review. *Biotechnol. Biofuels* **2021**, *14*, 154. [[CrossRef](#)]

Disclaimer/Publisher’s Note: The statements, opinions and data contained in all publications are solely those of the individual author(s) and contributor(s) and not of MDPI and/or the editor(s). MDPI and/or the editor(s) disclaim responsibility for any injury to people or property resulting from any ideas, methods, instructions or products referred to in the content.